SCREENING OF NATURAL DYES FOR USE IN DYE SENSITIZED SOLAR CELLS

DESALEGN JARA GODIBO

A thesis submitted to

The Materials Science program

Presented in Partial Fulfillment of the Requirements for

the Degree of Master of Materials Science

Addis Ababa University

Addis Ababa, Ethiopia

June 2012

Addis Ababa University

School of Graduate Studies

This is to certify that the thesis prepared by Desalegn Jara, entitled: *Screening of Natural Dyes for Use in Dye Sensitized Solar Cells* and submitted in partial fulfillment of the requirements to the degree of Degree of Master of materials science and complies with the regulations of the University and meets the accepted standards with respect to originality and quality.

Signed by the Examining Committee:

Examiner: Javed Mazher (Prof.) Signature _____ Date 25.06.2012

Examiner: B. Tilak (Dr.) Signature _____ Date 25-06-2012

Advisor: Teketel Yohannes (Prof.) Signature _____ Date 25/06/2012

_____

Chair of Department or Graduate Program Coordinator

Abstract

Screening of Natural Dyes for Use in Dye Sensitized Solar Cells

Desalegn Jara

Addis Ababa University, 2012

Five natural dyes, extracted from natural materials such as flowers, were used as sensitizers to fabricate dye-sensitized solar cells (DSSCs). Dye-sensitized solar cells (DSSCs) were fabricated using natural dyes extracted from flowers *Amaranthus caudatus*, *Bougainvillea spectabilis*, *Delonix regia*, *Nerium oleander*, *Spathodea companulata* and a mixture of the extracts. The PEC performance of the DSSCs based on these dyes showed that the fill factors of these DSSCs are mostly higher than 50%, the open circuit voltages (V_{OC}) varied from 0.45 to 0.55 V, and the short circuit photocurrent densities (J_{SC}) ranged from 0.013 to 1.82 $mAcm^{-2}$. Specifically, a high open circuit voltage (V_{OC} = 0.55 V) and short circuit photocurrent density (J_{SC} = 1.82 $mAcm^{-2}$) were obtained from the DSSC sensitized by the ethanol extract of flower of *Amaranthus caudatus*. The photon to electricity conversion efficiency of the dye-sensitized solar cell (DSSC) sensitized with the ethanol extract of flower of *Amaranthus caudatus* reached 0.61%. The PEC performances of DSSCs using the dye mixed solutions were also investigated. However, the mixed extract does not show synergistic photosensitization compared to the individual extracts. Instead, the cell sensitized by the flower of *Amaranthus caudatus* extract extracted with ethanol alone showed the best sensitization. The devices showed that an incident monochromatic photon to current conversion efficiencies (IPCE) varied from 4.7% to 52% illuminated from front side. The results from the IPCE data are consistent with the results from the current density – voltage (J − V) curves.

Acknowledgements

I offer my deepest gratitude and special affection to my advisor Prof. Teketel Yohannes for giving me an interesting research topic, his generous advice, devoted assistance, encouragement in all stages of the work, constant guidance and constructive criticism which were necessary for the progress of the research.

I would like the dearest and greatest thanks to my mother Angale Assaye for invaluable understanding, support and encouragement during the work. I would also like to thank especially the fantastic people in the laboratory Ato Sisay Tadesse and Ato Getachew Adam for the pleasant working environment and their helping hand in practical problems.

I am grateful to Arba Minch University for sponsoring me to join the school of graduate studies and continuous support my study. I appreciate the materials science program and the department of chemistry, Addis Ababa University, and staff members for their sincere cooperation during my study.

Finally, I would like to express my sincere thanks to my loved friends Eurisalem Kebede and Eyob Daniel who gave me fruitful suggestion during the whole work.

Table of Contents

List of Figures

List of Tables

1. INTRODUCTION

The world's energy consumption is continuously increasing and this creates a heavy demand for renewable energy sources to be developed. The largest challenge for our global society is to find ways to replace the slowly but inevitably vanishing fossil fuel supplies by renewable resources and, at the same time, avoid negative effects from the current energy system on climate, environment, and health. The worldwide power consumption is expected to double in the next three decades because of the increase in world population and the rising demand of energy in the developing countries [1]. This implies enhanced depletion of easily utilizable fossil fuel reserves in near future, leading to further aggravation of the environmental pollution. The reserves of fossil and even nuclear fuel are also limited: for example, the constantly rising gas prices give indication that the exhaustion of crude oil in the future. Solar energy is expected to play a crucial role as a future energy source. More solar energy strikes the earth in one hour (4.3×10^{20} J/hour) than all the energy consumed on the earth in a year (4.1×10^{20} J/year) [1]. Solar energy provides clean abundant energy and is therefore an excellent candidate for a future environmentally friendly energy source.

There are various types of solar cells that convert sun light in to electrical energy. For example, dye-sensitized solar cell (DSSC), the subject of the present thesis consist of a dye molecules attached onto the wide band semiconductor material that act as light absorbers and the counter electrode coated with a material capable of catalyzing the redox couple reaction in the electrolyte to decrease the charge transfer resistance.

The history of dye sensitized solar cells (DSSC) started in 1972 with a chlorophyll sensitized zinc oxide (ZnO) electrode [2]. For the first time, photons were converted into an electric current by charge injection of excited dye molecules into a wide band

gap semiconductor [2]. In the following years a lot of fundamental research was done on ZnO-single crystals [3, 4], but the efficiency of these devices was poor. The main problem was that a monolayer of dye molecules on a flat surface can only absorb up to 1% of the incident light [5]. A solution to this problem, developed by the Grätzel group, was to use a porous nanocrystalline TiO_2 electrode structure in order to increase the internal surface area of the electrode to allow large amount of dye to be contacted at the same time by the TiO_2 electrode and the electrolyte. By the successful combination of nanostructured electrodes and efficient charge injection dyes Grätzel and his co-workers developed a solar cell with energy conversion efficiency exceeding 7% in 1991 [5] and 10% in 1993 [6]. The research activity as well as the industrial interest in this technology is growing fast. DSSCs or Grätzel cells have attracted much attention in recent years due to their low-cost, simple, energy-efficient manufacturing, and use non-toxic and recyclable materials.

In this study we have extracted natural dye pigments from five locally available flowers namely *Amaranthus caudatus* (colour of the flower: deep red), *Bougainvillea spectabilis* (colour of the flower*:* deep red)*, Delonix regia* (colour of the flower*:* red)*, Nerium oleander* (colour of the flower: rose) and *Spathodea campanulata* (colour of the flower: red). We studied their photo-responses as sensitizers for dye-sensitized solar cells.

2. BACKGROUND

2.1 Design and Working Principles of the DSSC

The DSSC is composed of two electrodes, the working electrode (WE) and a counter electrode (CE). The working electrode consists of a dye sensitized mesoporous film attached to a conducting substrate. The conducting substrate is usually a glass plate coated with a thin layer of a transparent conducting oxide, such as fluorine doped tin oxide (F:SnO_2) or indium doped tin oxide (ITO). The opposite substrate to the TiO_2 layer, the counter electrode, is coated with a material capable of catalyzing the redox reaction in the electrolyte to decrease the charge transfer resistance. The void between the electrodes is filled with an electrolyte containing the redox couple. Electricity is generated on the photoelectrode, which is a nanoporous TiO_2 film sensitized with a monolayer of visible light absorbing dye and penetrated with a redox electrolyte (see Figure 2.1).

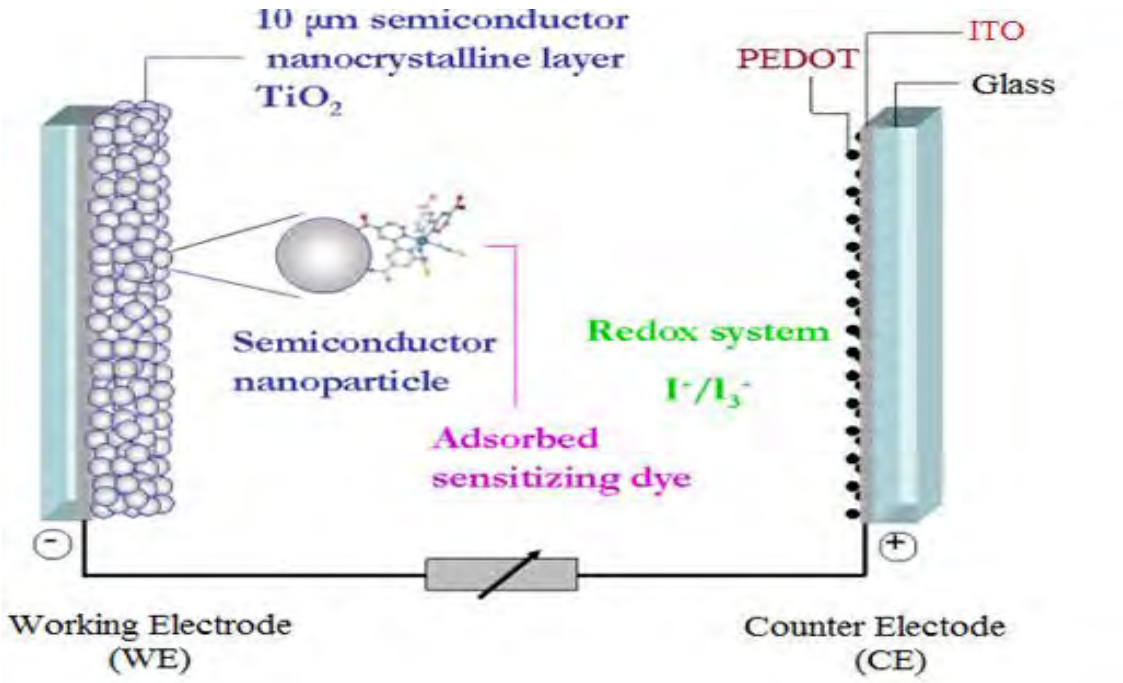

Figure 2. 1: Schematic illustration of the Dye Sensitized Solar Cell.

Having this construction, a TiO_2 electrode typically 10 μm thick, with an average particle (as well as pore) size typically in the order of 20 nm, has an internal surface area thousands of times greater than the geometrical (flat plate) area of the electrode [5]. Due to the large band gap of TiO_2 (E_g = 3.0 - 3.2 eV), it only absorbs light in the UV-region of the solar emission spectrum.

The regenerative working cycle of the dye-sensitized solar cell is depicted in Figure 2.2, showing schematically the relative energy levels of DSSC. Under illumination the incoming photon is absorbed by the dye molecule adsorbed on the surface of the nanocrystalline TiO_2 particle and an electron from a ground state, S^0, of the dye molecule is excited to a higher lying excited state, S*. The excited electron is injected to the conduction band of the TiO_2 particle leaving the dye molecule to an oxidized state, S^+, which means it has one less electron before. In order for the current generation to continue, the dye must be reduced back to its ground state. This is done by the redox couple in the electrolyte and causes the redox mediator to become oxidized. After injection, an electron diffuse in the nanocrystalline TiO_2 network and eventually reaches the back contact of the working electrode where charge collection and charge extraction occurs. The extracted charge can subsequently perform electrical work in the external circuit and reaches the counter electrode, where reduction of the redox mediator takes place which means when the original lost electron reaches the counter electrode, it gives the electron back to the electrolyte.

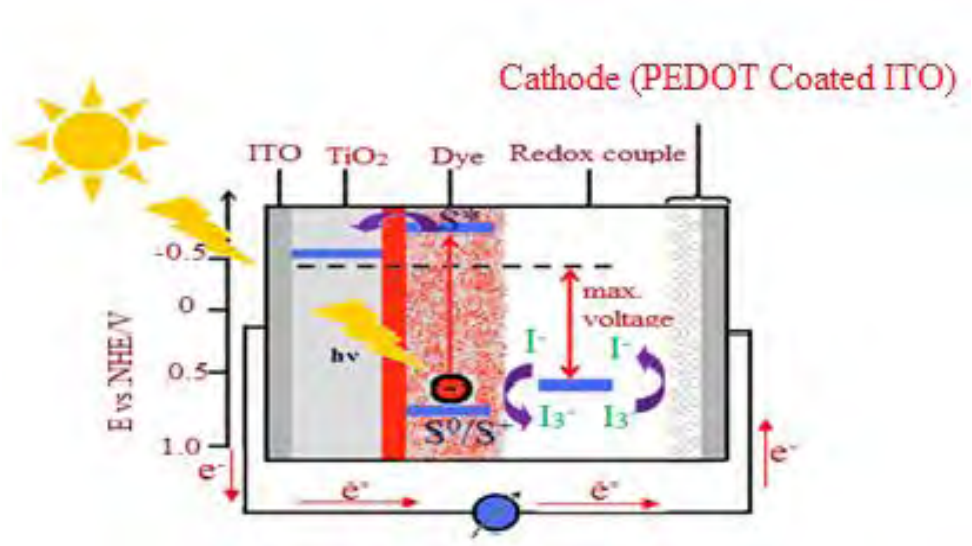

Figure 2. 2: Schematic illustration of the electron flow in DSSC.

The chemical reactions going on in the photoelectrochemical (PEC) cell can be summarized as follows [7]:

At the photoelectrode:

•Light absorption: $2S^{O}(dye) + 2hv \rightarrow 2S^{*}$ (1)

•Electron injection: $2S^{*} \rightarrow 2S^{+}2e^{-}(TiO_2)$ (2)

•Dye reduction: $2S^{+} + 3I^{-} \rightarrow 2S^{O} + I_3^{-}$ (3)

•Overall: $3I^{-} + 2hv \rightarrow I_3^{-} + 2e^{-}(TiO_2)$ (4)

At the counter electrode:

• Reduction of the redox mediator: $I_3^{-} + 2e^{-} \rightarrow 3I^{-}$ (5)

Where S^0 = the ground state of the dye; S* = the excited state of the dye; S^+ = the oxidized state of the dye.

Due to the energy level positioning in the system, the photoelectrochemical (PEC) cell is capable of producing voltage between its electrodes and across the external load. The maximum theoretical value for the photovoltage at open circuit condition is

determined by the potential difference between the conduction band edge of the TiO_2 and the redox potential of the electrolyte [8]. The operation of the cell is regenerative in nature, since no chemical substances are neither consumed nor produced during the working cycle.

2.2 Operation Principle of DSSC

The operation of a photovoltaic cell can be generally fall into three basic steps: light absorption, charge separation and charge collection. The physical or chemical processes behind these principal steps vary between different types of solar cells and photovoltaic materials. The efficiency of a solar cell depends on the efficiency of each of these steps and is maximized by the materials selection and the cell design.

2.2.1 Light Absorption

While the high efficiency of the dye sensitized solar cell arises from a collective effect of numerous well-tuned physical and chemical nanoscale properties as will become apparent later, the key issue is the principle of dye-sensitization of large band-gap semiconductor electrodes. As already mentioned, in the DSSC this is accomplished by coating the internal surfaces of the porous TiO_2 electrode with special dye molecules tuned to absorb the incoming photons. The adsorption of the dye to the semiconductor surface usually takes place *via* special anchoring groups (e.g. carboxylate, phosphonate or hydroxamate) attached to the dye molecule. The absorption of a photon by the dye molecule happens *via* an excitation between the electronic states of the molecule. Photon absorption induces an electronic transition between the HOMO (highest occupied molecular orbital) and LUMO (lowest unoccupied molecular orbital) of the dye.

2.2.2 Charge Separation

The charge separation in DSSCs is based on an electron transfer process from the dye molecule to TiO_2 and a hole transport process from the thereby oxidized dye to the electrolyte. Efficient charge separation is, on the other hand, achieved because the electrons and holes travel in different mediums – this prevents bulk recombination which is a problem in conventional p-n junction cells.

The electron transfer mechanism is strongly dependent on the electronic structure of the adsorbed dye molecule and the energy level matching between the excited state of the dye and the conduction band of the TiO_2.

While charge separation in the semiconductor p-n junction arises from the electric field in the space-charge layer in the junction area, space charge occurs when two different semiconductor materials are brought together. Electrons very near the interface in one of the materials (the donor) typically migrate in the other material (the acceptor) in order to establish thermodynamic equilibrium. Atoms that lose electrons are positively charged and form a fixed space charge layer within the donor. The situation in a nanoparticle electrode - electrolyte interface is quite different. The individual particle size in the nanostructured electrode, typically a few tens of nanometers, is too small for the formation of a space charge layer inside the particles [9].

Furthermore, no significant macroscopic electric fields are present between the individual nanoparticles in the bulk of the electrode. In this case, the absence of band bending is a result of the individuality of each nanocrystalline particle. In general, bands will bend locally when materials come in contact; because the two Fermi levels of the materials will equilibrate to the same level through a local exchange of charge

carries (either holes or electrons).This exchange of charge changes the energies of those charge carriers who have been exchanged. A sufficiently thick nanoparticle film could have a collective space charge, if the film behaved as an ensemble. However, the electrolyte surrounding all the particles effectively decouples the particles and screens any existing electric fields within about a nanometer [10].

The major mechanism for the charge separation is however the energy level positioning between the dye molecule and the nanoparticle. The excited state of the dye (the LUMO level) is slightly above the conduction band edge of the TiO_2 and the dye's HOMO level is slightly below the chemical potential of the redox pair in the electrolyte, both presenting an energetic driving force for the electron and hole separation.

2.2.3 Charge Transport

In the DSSCs charge transport happens by electron transport in the nanostructured TiO_2 electrode and hole transport in the electrolyte. Both charge transport mechanisms are equally important for the operation of the solar cell.

The semiconductor nanoparticle network works not only as a large surface area substrate for the dye molecules but also as a transport media for the electrons injected from the dye molecules. Because of the porous structure of the electrode and the screening effect of the electrolyte, the electrode can be viewed as a network of individual particles through which electrons percolate by hopping from one particle to the next [11]. As mentioned above, the small size of the particles prevents the formation of a space charge layer and a built-in electric field inside the particles, and therefore the transport of electrons cannot be drift in an electric field. Recombination processes being efficiently blocked at the semiconductor electrolyte interface the

generation of electrons to the conduction band of the TiO_2 particles under illumination results in an electron concentration gradient in the electrode and the electrons are transferred to the TCO back contact layer by diffusion.

Measurements have shown that the diffusion of electrons is characterized by a distribution of diffusion coefficients, which have been related to hopping of electrons *via* surface traps of different depths [11]. These electron traps are localized energy states just below the conduction band edge of the TiO_2 and they play a significant role in the electron transport. Because of the majority carrier nature of the TiO_2 electrode, trapping of electrons in the bulk states does not lead to recombination losses. Instead trapping of electrons at the TiO_2 surface may be a pathway for recombination, resulting in photocurrent losses and also photovoltage losses for kinetic reasons [9].

The diffusion coefficient of electrons depends on the electron quasi-Fermi level under illumination. A quasi Fermi level is the new Fermi level that describes the population of each type of charge carrier (electrons and holes) in a semiconductor separately when their populations are displaced from equilibrium. This displacement could be caused by exposure to light of energy $E > E_g$, which increases the density of both electrons and holes above their equilibrium values. At low light conditions only deep traps participate in the electron transport causing a low diffusion coefficient. Increasing the light intensity raises the electron quasi-Fermi level and deep traps are filled at steady state condition, while shallow traps contribute to the electron motion, resulting in a larger diffusion coefficient [11]. Increasing the illumination level thus increases the conductivity of the TiO_2 electrode by filling the trap states.

It has also been suggested that the motion of the electrons in the semiconductor particles is coupled to the species in the electrolyte at the semiconductor-electrolyte

interface [11]. The electron transfer process at the metal oxide electrode/electrolyte interface is important to the operation of photoelectrochemical cells, because nanoparticulated TiO_2 films with an enhanced surface area cause the formation of a large number of electron traps at the nanostructured semiconductor/electrolyte interface, such as at the intrinsic defect sites (e.g. oxygen defects or surface states) and the grain boundaries, which may influence the interfacial charge-transfer kinetics [12, 13].

The properties of nano-sized materials are different from those of the same materials in the bulk state. First, the surface to volume fraction is increased in accordance with the size reduction of the particles [14]. This means that surface related defects play an important role in determining the electronic energy levels of an electrode composed of metal oxide nanoparticles. Second, the composed small-sized nanoparticles cannot induce a significant amount of band bending, keeping electric neutrality by surrounding electrolyte with high concentration thereby resulting in the lack of a potential barrier at the interface between the semiconductor electrode and electrolyte [15]. Therefore, concentration gradients (diffusive transport) rather than the electric field (drift transport) contribute to the electron transport in the electrode/electrolyte interface [16]. In the nanoparticulated TiO_2 system, electron transportation is strongly affected by trapping and detrapping events [17]. Electron transfer across a semiconductor/electrolyte interface influences the surface electronic states of a nanoporous metal oxide electrode. Surface states originate from the breakdown of the lattice periodicity in the semiconductor, resulting in the formation of the rearrangement of the surface atoms.

Understanding the mechanisms of charge transport in the nanostructured electrode electrolyte systems is important for the further development of the dye-sensitized nanostructured solar cell concept.

2.2.4 Recombination

Recombination of the generated electrons with holes in the dye-sensitized nanostructured TiO_2 electrode can in principle occur either after the electron injection or during its migration in the TiO_2 electrode on its way to the electrical back contact.

Illumination of the dye-sensitized electrode initially in equilibrium (in the dark) generates a transient electric field between the injected electrons in the TiO_2 and the oxidized species in the electrolyte. This electric field could in principle oppose further charge separation and promote recombination. However, in the dye cell the mobile ions in the electrolyte can easily rearrange and effectively screen the light induced opposing fields in steady state conditions throughout the electrode film, and thus enable an efficient charge separation [18].

In the silicon solar cells the recombination of charge carriers in trap states in, surfaces, grain boundaries, and in the bulk degrades the cell performance easily, and thus semiconductor material of high crystal purity is required. In the dye-sensitized TiO_2 electrode, there is on the contrary vast amount of particle boundaries and a huge surface to volume ratio. Yet the dye solar cell does not seem to suffer from the recombination losses at the grain boundaries at all. The reason for this is that only electrons are transported through the semiconductor particles, while holes (oxidized ions) are carried by the electrolyte.

2.2.5 Interfacial Kinetics

The dye-sensitized solar cell is based on photoelectrochemical reactions at the semiconductor-electrolyte interface, as already discussed, and the operation of the cell is therefore an outcome of competing opposite chemical reactions having different rate constants. A desired direction of the electrochemical reactions is achieved with fast wanted reactions (high rate constants) and slow unwanted reactions (low rate constants).

For a conventional DSSC, based on a ruthenium dye, typical time constants for the different interfacial electron-transfer processes are summarized in a highly simplified manner in Figure 2.3. The electron injection has been reported to occur in less than 100 fs to 100 ps depending on the experimental conditions [19]. The electron injection is significantly faster than the de-excitation of the dye that occurs in ~20 ns [19]. The recombination of electrons in the TiO_2 with the oxidized dye or the redox electrolyte occurs in micro-milliseconds (μs-ms) and competes with the regeneration of the dye that occurs in ~ μs [20, 21]. The desired reaction, the electron injection from the excited state of the dye to the conduction band of TiO_2, exceeds any unwanted reaction in an order of magnitude or more. In fact, occurring in the femtosecond time scale, the electron injection process between the dye and TiO_2 in the DSSC is one of the fastest chemical processes. Another desirable reaction, the regeneration of the dye is also a very fast reaction occurring in 0.1μs in the normal conditions in the DSSC. This is important for obtaining high cycle life for the dye, since lack of adequate conditions for the regeneration leads to dye degradation [11]. The interfacial electron-transfer kinetics varies with the nature of the components.

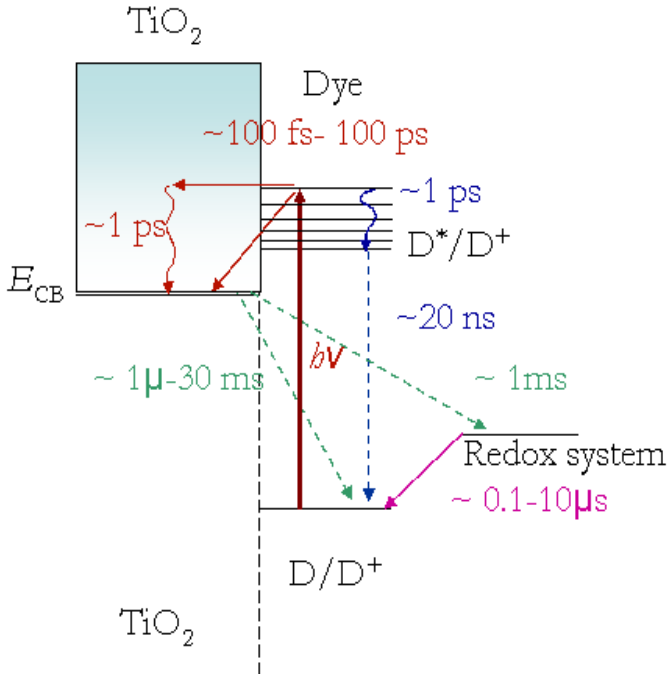

Figure 2.3: Illustration of the interfacial electron-transfer kinetics in DSSCs based on conventional ruthenium based dyes.

2.3 DSSC Basic Materials and Manufacturing Methods

2.3.1 Substrates

Requirements for a good DSSC substrate are low sheet resistance which should also be independent of temperature up to 450 – 500°C (in case when the electrode post-treatment requires sintering), high transparency, and ability to prevent impurities such as water and oxygen from entering into the cell. The traditional approach is to build the DSSC on transparent conducting oxide (TCO) coated glass sheets. The most often used TCOs are fluorine- and indium-doped tin oxides, whose sheet resistances are around 10 Ω/sq. Whilst glass is obviously an effective barrier towards water and oxygen penetration into the cell, its disadvantages are fragility, rigidity, heavy weight and high price. ITO's sheet resistance also increases with temperature so ITO-coated glass is not the best option for cells where high temperature treatments are needed.

Alternative substrate materials such as plastic foils and metal sheets overcome most of the glass' problems. Conductive plastics, like ITO-PET (indium doped tin oxide coated polyethylene terephthalate) and ITO-PEN (indium-doped tin oxide coated polyethylenenaphtalate), are light weight and flexible, whereas metals are also mechanically robust, cheap, and their electrical conductivity is superior compared to all other substrate materials. The last factor plays a crucial role in cell size upscaling, since the main part of the total Ohmic losses in the cell are due to lateral resistance on the substrate surface. It has also been noticed that substrate-mediated recombination is lower from stainless steel than from glass [22]. Disadvantages of plastics include low temperature tolerance, maximum 150 – 160^{o}C, for ITO-PET high sheet resistance, around 60 Ω/sq, and uncertainties considering the oxygen and water penetration. For metals, the main problem is the traditionally used, iodine-containing electrolyte. Triiodide ions are corrosive, and thus far only stainless steel and titanium have shown enough chemical stability in the iodine electrolyte to be successfully employed as DSSC substrates [23, 24]. Long-term stability of metal-based cells is still unknown, though, and requires further studies before this DSSC type can be transferred to large scale manufacturing. However, the main spur behind the alternative substrate research is the flexibility of both the plastic and metal substrates which potentially leading to high volume production of low cost solar cells with wide variety of applications.

2.3.2 Photoelectrode

The semiconductor material that forms the core of the photoelectrode (PE) should be chemically stable and inert towards the electrolyte species, it should have a lattice structure suitable for dye bonding, its conduction band should be located slightly below the LUMO level of the dye in order to facilitate efficient electron injection, and

it should be available in nanostructured form to enable high enough dye loading. Titanium dioxide fulfills these requirements – in addition to that, it is also cheap and easily available because of mass production. Another semiconductor oxide that has been employed in the DSSC is zinc oxide but there have been problems for example with the dye desorption [25] which is why TiO_2 is still the most widely used DSSC photoelectrode material.

TiO_2 exists naturally in three crystalline forms; anatase, rutile, and brookite. The TiO_2 powder used for the making of the thin film is composed of rutile and/or anatase. For DSSC, however, the preferred crystal form is anatase due to its large band gap of 3.2 eV and higher conduction band edge, which results in a higher Fermi level and open circuit voltage. The densities are 3.89 g/cm^3 and 4.26 g/cm^3 for anatase and rutile, respectively. The third crystalline form of TiO_2, brookite, is difficult to produce and is therefore not of practical interest for the dye solar cells. The typical TiO_2 nanoparticle size in the photoelectrode (PE) film is 10 – 30 nm, though larger particles up to 300 – 400 nm are sometimes added to the film to increase the path length of the absorbed photons by scattering (improved light harvesting efficiency). The optimal photoelectrode film thickness is 10 – 15 μm – if the film is very thin the dye loading remains too low whereas with too thick films, the distance the excited electrons generated on the electrolyte side of the photoelectrode film have to travel before reaching the current collector becomes so long that increased recombination probability starts to decrease the cell efficiency.

Screen-printing is a typical TiO_2 layer deposition method, with which large quantities of even quality films can be prepared with high speed (on laboratory scale, technique called “doctor-blading”, in which the TiO_2 precursor is applied through a hand-cut tape mask is often employed). Several research groups prepare their own TiO_2

precursor materials but there exists also commercial titania pastes specifically designed for screen-printing technique – in addition to the TiO_2 nanoparticles they contain some high viscosity organic solvent, binders, pH-adjusting agents, and morphology controlling agents. After the film deposition the solvent and other organic ingredients have to be removed, which is done by sintering the film in 450 – 500^{o}C for half an hour minimum. In this treatment the individual TiO_2 nanoparticles also "neck" together and adhere more tightly to the substrate surface which decreases the interparticle resistance, thus facilitating efficient electron diffusion in the film, and the resistance for the electron transfer from the TiO_2 network to the substrate. Unfortunately, this sintering treatment, which drastically improves the TiO_2 film quality and also its mechanical stability, cannot be employed with plastic substrates, due to their low temperature tolerance. One promising technique for low temperature photoelectrode film preparation is spraying suspension of TiO_2 nanoparticles in high volatility solvent (e.g. ethanol) on heated substrate and then mechanically compressing the resulting powder layer. Titania pastes suitable for low temperature sintering have also been developed but the problem of inadequate interparticle necking and thus lower cell efficiency, due to slower electron transport in the film and thus higher recombination probability, still remains with these materials too.

Dye sensitization of the photoelectrode (PE) is done simply by soaking the TiO_2 film in the dye solution, the soaking time typically being overnight minimum, though the process can be speed up by heating the solution. The dye is one of the most expensive components of the cell, due to the complex structure and demanding, multistep synthesis of the molecule, but since its amount in the solution is very small, typically of the order 10^{-4} M, its effect on the overall manufacturing costs of the cell remains reasonably low. In addition to the ruthenium organometallic complexes, other dyes

such as coumarins, eosins, perylenes and natural dyes extracted from plants have been employed in the DSSC, though the highest efficiencies have still been obtained with the Ru-complexes. As a matter of fact, the molecular structure of the dyes and the electron transfer processes in the dye excitation resemble those of the chlorophyll molecule in green plants, which is why the DSSC operating principle has sometimes been called “artificial photosynthesis”.

2.3.3 Electrolyte

In addition to the redox couple – like the most commonly used iodide/triiodide – the electrolyte usually contains some “blocking agent” that adsorbs on the photoelectrode on those surface sites not occupied by the dye to prevent recombination, i.e. electron leakage from the TiO_2 back to the electrolyte. 4-tert-butylpyridine, guanidinium thiocyanate and 4- guanidinobutyric acid are some molecules used for this purpose [26]. Due to suppressed recombination, the cell open circuit voltage increases. The requirements for the electrolyte solvent are its ability to dissolve the other ingredients and preferably low volatility combined with high viscosity to facilitate fast ionic diffusion between the electrodes. Typical solvents used in the DSSC electrolyte are various nitriles (aceto-, methoxypropio-, valero-, butyro-), carbonates (ethyl-, propyl-) and their mixtures. Liquid electrolyte can also be gelatinized, for example with certain polymers (Example: polyvinylidenefluoride-hexafluoropropylene (PVDF-HFP) or silica nanoparticles [27]. While this does not remove the problem of the cell “drying” in case of structural damage to the substrates, it does prevent electrolyte leakage. Obviously, the liquid electrolyte is the weak link considering the cells’ long-term stability which is why solid hole conductors such as copper iodide (CuI), copper thiocyanate (CuSCN), copper bromide (CuBr) complexes, 2,2′7,7′-tetrakis-(N,N-di-p-

methoxyphenyl-amine)-9,9′-spirobifluorene (spiro-MeOTAD), and the conducting polymer poly(3,4-ethylenedioxythiophene) (PEDOT) have also been studied as its replacement [28 - 30]. Among them, polymer gel electrolytes are considered as one of the most prospective substitutes for liquid electrolytes to fabricate practical applicable quasi-solid-state dye-sensitized solar cell due to their merits such as high ionic conductivity, good interfacial filling property, and relatively high long-term stability. Either the cell efficiency or its stability have not been satisfactory with these – one reason being the solid material's poor penetration into the pores of the TiO_2 layer – which is why iodine-based liquid electrolyte is still the most often used alternative in the DSSC. An example of a typical electrolyte composition is 0.5 M lithium iodide (LiI), 0.05 M iodine (I_2), and 0.5 M 4-tert-butylpyridine in 3-methoxypropionitrile (triiodide ions are generated in a reaction of molecular iodine with the iodide ions). The amount of iodine may vary according to the electrolyte layer thickness.

There is also an interesting, new group of DSSC electrolytes in which so-called ionic liquids or room temperature molten salts are utilized [31]. Ionic liquids are fluids with no vapor pressure at all which eliminates the problem of electrolyte drying in case of fractures on the substrate. Typically, ionic liquids are salts of iodine with a large, often imidazole-based cation, for example 1-methyl-3-propylimidazolium iodide (PMII) or 1, 2- dimethylimidazolium iodide (DMPII). Thus, ionic liquid works as a source of iodide ions and also as a solvent, due to its fluidic nature. The problem of these electrolytes is, however, the high viscosity of many ionic liquids, which slows down the ionic diffusion and tends to keep cell efficiencies down. Some ionic liquids are also hygroscopic which means that special conditions e.g. dry air or nitrogen atmosphere is needed for cell preparation and storage of materials.

2.3.4 Counter Electrode (CE)

For DSSCs deposited on glass, thermally deposited or sputtered platinum is the most widely used CE catalyst. The advantages of Pt are its high catalytic activity towards the iodide/triiodide redox reaction which is why only a few nanometer layer of Pt is required – this keeps the cell manufacturing costs low even if Pt is an expensive element, and because the thin Pt layer is almost transparent, platinized counter electrodes can be employed also in cells which require reverse lighting (i.e. lighting from the CE side). Platinum is also chemically stable in the electrolyte, i.e. no remarkable dissolution over time from the CE have been noticed (in case the CE catalyst dissolves and diffuses to the PE, it may act as recombination centers, thus decreasing the cell efficiency). In the thermal method, an alcoholic solution of platinum salt (e.g. $PtCl_4$ or H_2PtCl_6) is spread on the substrate and after the solvent evaporation; the substrate is fired in an oven in 385^{o}C for about 15 minutes. This results in reduction of metallic platinum as tightly adhered nanoscale clusters on the substrate surface [32]. Due to high temperature involved, this method is naturally not suitable for plastic substrates but sputtering, which is a well known and widely applied method for thin film coatings, can be employed for low temperature tolerance substrates as well.

Since platinum is an expensive catalyst, even if the consumption is relatively low, other materials such as nanostructured and/or activated carbon and conducting polymers such as PEDOT or PANI (polyaniline) have been studied as its replacement [33]. The main problem with these materials is that often rather thick layers of them are needed in order to reach high enough catalytic activity. This slows down the cell

manufacturing process and, as thick catalyst layers also absorb light, these kinds of CEs are not suitable for reverse lighting cells.

2.3.5 Dye

The most speciality of the DSSC relative to the other types of solar cells is the use of the dye. It's well known that the energy gap size of the applied semiconductors determines the absorption frequency of light in the solar cells. A significant purpose for using the dyes in the DSSC is to expand the absorption spectra on the visible light due to the visible light possess about 96% energy of the sun light [34]. The absorption spectra of the DSSC are decided by the combination of the photoelectrode's nanoparticles, e.g. TiO_2, and the dyes, where the dyes can help the DSSC to expand their absorption spectra.

The efficient spectral sensitization in the DSSC is made evident in Figure 2.4, where the spectral response curves, i.e. the photon to current efficiency curves, for cells sensitized with different dyes is compared with a naked TiO_2 electrode. The actual sensitization effect can be seen in Figure 2.4 as a shift of the IPCE curve of the naked TiO_2 to the higher wavelengths when coated with the dye [35]. The current efficiency of the cell is related to the 'height' of the IPCE curve, which depends on the charge separation and charge collection efficiencies. The IPCE curves in Figure 2.4 are not corrected for the optical losses in the glass substrate, which only makes the obtained peak IPCE values more significant.

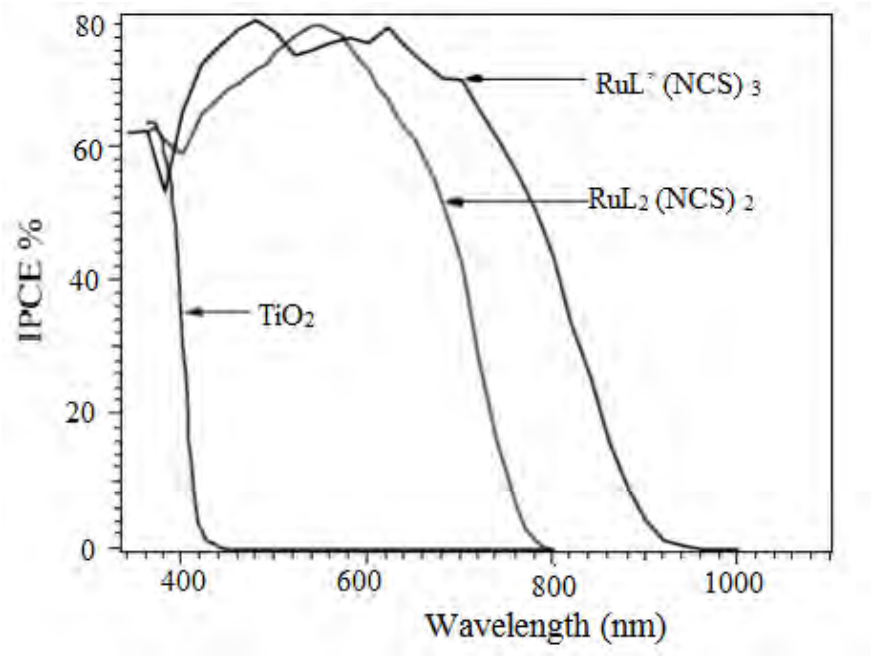

Figure 2. 4: Spectral response (IPCE) of dye-sensitized solar cell for the N_3 (ligand L = 4, 4'-COOH-2, 2'-bipyridine) and the black dye (ligand L' = 4, 4', 4" -COOH-2, 2':6', 2"-terpyridine) compared with the spectral response of bare TiO_2 electrode.

A dye is essential to a photoelectrochemical solar cell with a large band gap semiconductor photoelectrode, in order to boost the efficiency of the cell. The photoelectrode semiconductor in itself may be practically transparent to visible and infrared light, which is the case with e.g. TiO_2. Therefore it is dyed for increased efficiency. The wider the part of the spectrum that can be absorbed, the more energy can be converted to electricity. Chlorophyll was a coloring agent alternative when research on dye sensitization grew in the 1970s. Since then, far more effective dyes have been discovered, the most successful of which are the ruthenium complex dyes.

Ruthenium dyes are frequently used since they so far are the most successful sensitizers in nanostructured thin film photoelectrochemical solar cells. Ruthenium is an expensive element though. If an alternative dye, such as a plant dye, could be made to perform as well as ruthenium dyes, it would be interesting for environmental and

economical reasons alike. Especially for investors in nanocrystalline thin film photoelectrochemical solar cells, with developing countries regarded as potential investors, it would be of economic interest to replace the ruthenium with cheaper dyes. A goal for the research on plant based dyes for photoelectrochemical solar cell use is to come up with a dye as effective as the ruthenium-based dyes. Whether or not it is economically capable to substitute plant dyes for ruthenium depends on the provided solar cell efficiency along with the long time stability of the dyes.

From an environmental point of view, substitutes for ruthenium would be preferable, as long as the substitutes are not even more toxic and detrimental to the environment. Even though a functional solar cell in use is not a threat to the ambient nature, undesired leakage or unsatisfactorily handling when the solar cell lifetime has expired, could cause environmental problems. For a photoelectrochemical solar cell to function under working conditions, it must be well sealed, for the electrolyte must not evaporate. Therefore, leakage of toxic components will not be a problem unless the solar cell is damaged. These economic and environmental issues justify the search for alternative dyes.

The dyes used in DSSCs can be divided into two categories: metal based complexes and metal-free organic dyes. The photovoltaic performances of ruthenium based complexes are still unsurpassed (11.1%). The high efficiencies of the ruthenium dyes based DSSCs can be attributed to their wide absorption range from the visible to the near- infrared region. Some of the superior ruthenium dyes up to date are N3 [35], N719 [36], Black dye [37], K19 [38] and K77 [39]. N3 is the pioneer dye reported in 1993 by Nazeeruddin et al. [6] and is depicted together with two other dyes also reported by the same group, see Figure 2.5. The later are hydrophobic alternatives that have shown improved light-harvesting efficiencies and long time stabilities [38, 39].

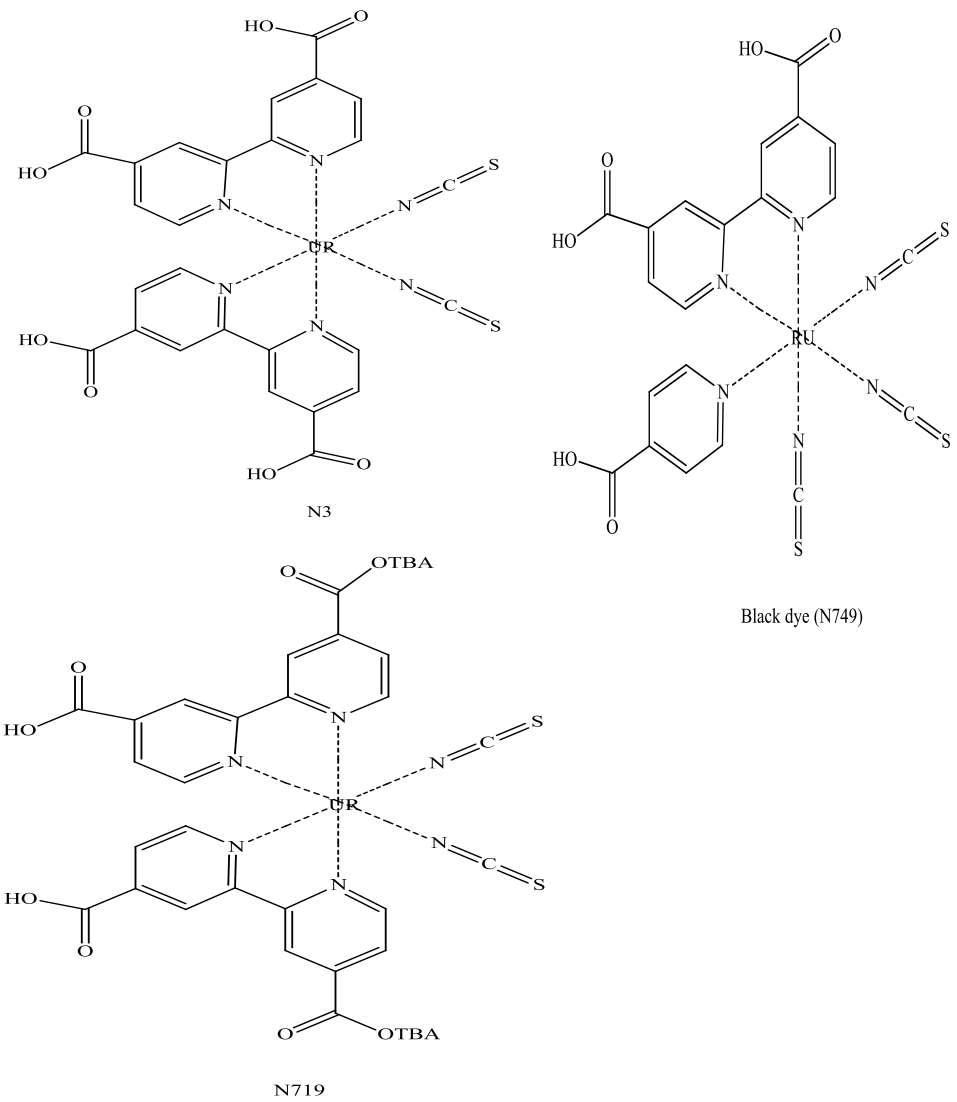

Figure 2. 5: The molecular structure of N3, N719 and black dye (N749).

From the year of 2000 the interest in organic dyes has steadily increased yielding record efficiencies from 4% to 9% for DSSCs based on fully organic dyes [40, 41]. The main advantages of organic dyes are the short established synthetic routes enabling fairly easy dye structural modifications. In addition, organic dyes usually show significantly higher extinction coefficients compared to metal-based complexes. As a consequence organic dyes have quite narrow absorption bands in comparison to metal based dyes. The high extinction coefficients of organic dyes reduce the amount of dye required for efficient light harvesting and make organic dyes suitable for thin TiO_2 films required for solid-state DSSCs. The structure of three well investigated

organic dye families, triphenylamine (TPA), coumarin and indoline, are shown in Figure 2.6.

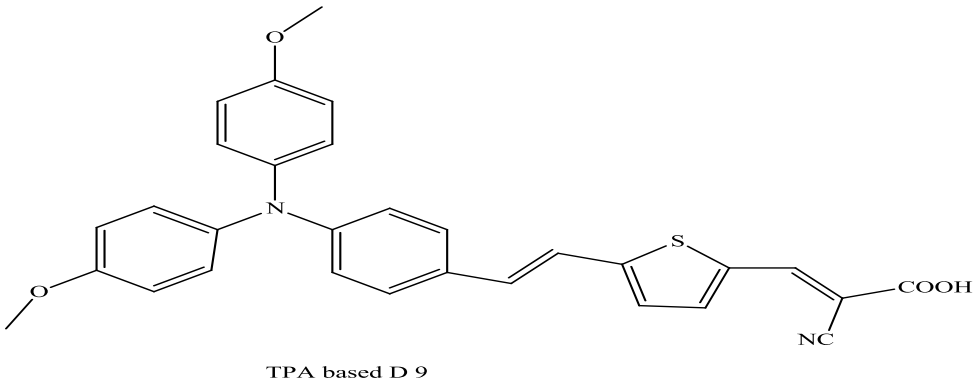

TPA based D 9

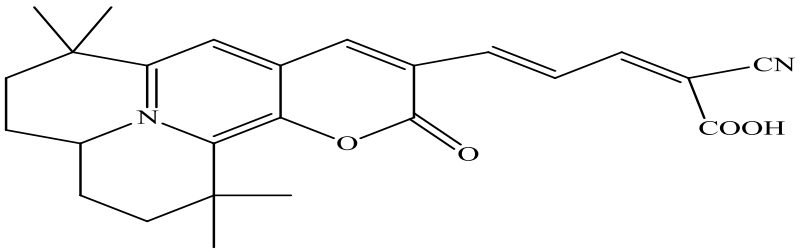

Coumarian based
NKX-2311

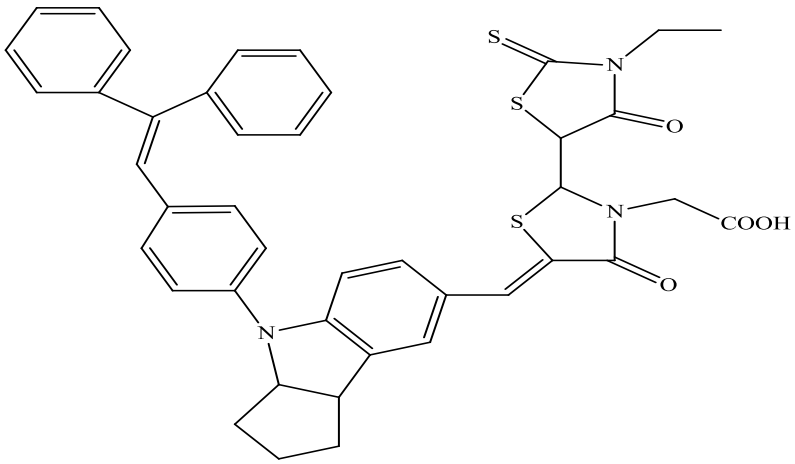

Indoline based D149

Figure 2. 6: The molecular structure of TPA based D9, coumarin based NKX-2311 and indoline based D149.

2.4 Pigments

2.4.1 Structures and Chromophores of Anthocyanins and Anthocyanidins

Anthocyanidins is a subgroup of the flavonoids, polyphenolic compounds possessing 15 carbon atoms: two benzene rings joined by a linear three-carbon chain [42]. Anthocyanidins are aglycons of corresponding anthocyanins, which are weak acids and occur naturally in a great many plants. The colours of anthocyanins are typically red, blue, violet, orange and pink [42]. Chromophores of anthocyanins absorb different parts of the visible and ultraviolet spectrum, depending not only on the type of anthocyanin, but also on the type of sugar attached, where on the carbon skeleton this sugar is attached, pH, complexes formed with metal cations and the presence of colourless flavonoids. There are more than 19 known naturally occurring anthocyanidins or aglycones based on the skeleton [43]. Among them, the six most common anthocyanidins in nature are cyanidin, pelargonidin, peonidin, delphinidin, petunidin, and malvidin. Anthocyanins as glycosides of anthocyanidin chromophores can be polyhydroxy and polymethoxy derivatives of 2-phenylbenzopyrylium (flavylium) salts linked with aromatic, aliphatic acids, and ethyl ester derivatives [44].

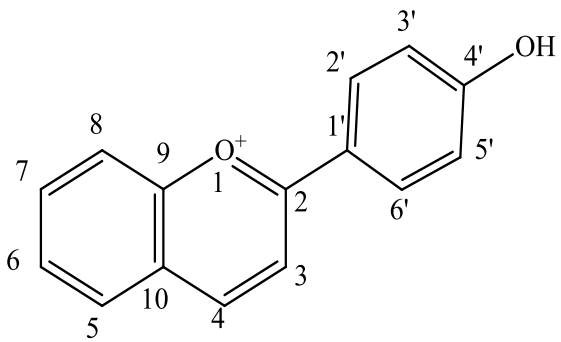

Figure 2. 7: Basic chemical structures of the most abundant anthocyanidins**.**

Table 2. 1: **The most common naturally occurring anthocyanidins.**

Name	Substitution						Colour
	3	5	6	7	3’	5’	
Pelargonidin	OH	OH	H	OH	H	H	Orange
Cyanidin	OH	OH	H	OH	OH	H	Orange-red
Delphinidin	OH	OH	H	OH	OH	OH	Bluish-red
Peonidin	OH	OH	H	OH	OCH_3	H	Orange-red
Petunidin	OH	OH	H	OH	OCH_3	OH	Bluish-red
Malvidin	OH	OH	H	OH	OCH_3	OCH_3	Bluish-red

Anthocyanins are water-soluble and found in vacuoles in plant cells of angiosperm families (flowering plants). The anthocyanins can be used as pH-indicators, as many of them change colour depending on the pH of their surroundings. Generally, anthocyanins adapt to changes in acidity (or alkalinity) according to this outline. In acidic environments the chromophore of anthocyanins is an aromatic flavylium (2-phenylchromenylium) cation, red in colour. In a more basic surrounding the double bond of the flavylium cation is disrupted by a water molecule, and the result is a colourless structure. This structure can regain colour under even more alkaline ambient conditions, since dehydroxylation restores a conjugated double bond in the anthocyanin structure. The key to this behaviour lies in the conjugated double bonds.

Conjugated double bonds make possible the absorption of photons of lower energy (and longer wavelengths) in the visible spectrum, i.e., with conjugated double bonds lower photon energies are required to excite electrons. The more extensive the system of conjugated double bonds, the lower energies can be accepted for excitation. When

a hydroxide is inserted into the structure, a double bond is broken and now the photon-energy required to excite an electron is higher than it was before the introduction of the hydroxide, so the absorption is pushed towards (and into) the ultraviolet. Conversely, removal of a hydroxide can restore double bonds and again lower the adequate excitation energy and bring the absorption back to visible regions [42]. Figure 2.8 shows the change in molecular structure and colour for cyanin for different pH-values. Anthocyanins are not very stable in alkaline environments, or in environments with a high sugar concentration [42].

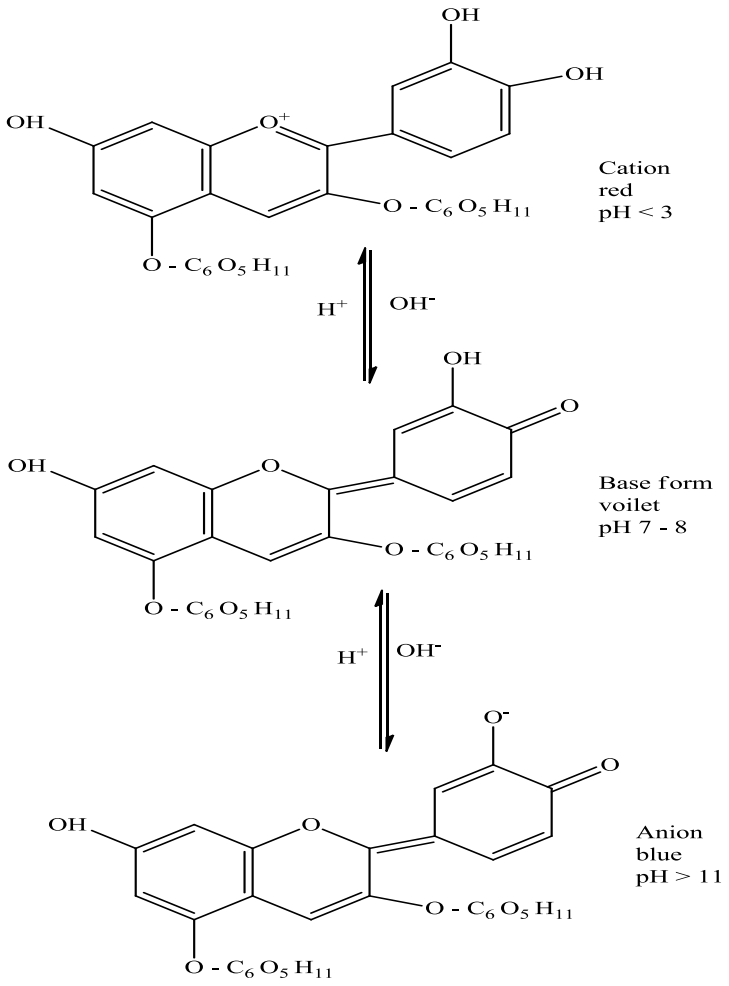

Figure 2. 8: The molecular structure and dependence of colour of cyanin on pH.

2.4.2 Betalains, Betacyanins and Betanins

Betanin is a type of betacyanin, which is a larger group of red-violet pigments, and betacyanins are in turn part of a larger group of pigments, known as betalains. Betalains are found in vacuoles of cells of families of plants belonging to the order Caryophyllales. It can be found in roots, fruits and flowers of these families [45]. A finding, which so far remains unexplained, is why plants containing betalains appear to be void of anthocyanins [42] and *vice versa*. The two pigment groups seem to perfectly exclude each other in the paths of evolution [45].

Betalains are water-soluble nitrogen-containing pigments, which are synthesized from the amino acid tyrosine into two structural groups: the red-violet betacyanins and the yellow-orange betaxanthins. Betaxanthins are conjugation products of betalamic acid with different amino acids or amines [46]. Betacyanins are immonium conjugates of betalamic acid with cyclo-DOPA (dihydroxyphenylalanine) [45]. Betalamic acid, whose structure is presented in Figure 2.9a, is the chromophore of betalains (betacyanins and betaxanthins) pigments [45]. The nature of the betalamic acid addition residue determines the pigment classification as betacyanin or betaxanthin (Figure 2.9b and 2.9c, respectively). Betanin: $R_1 = R_2 = H$. R_3 = amine or amino acid group.

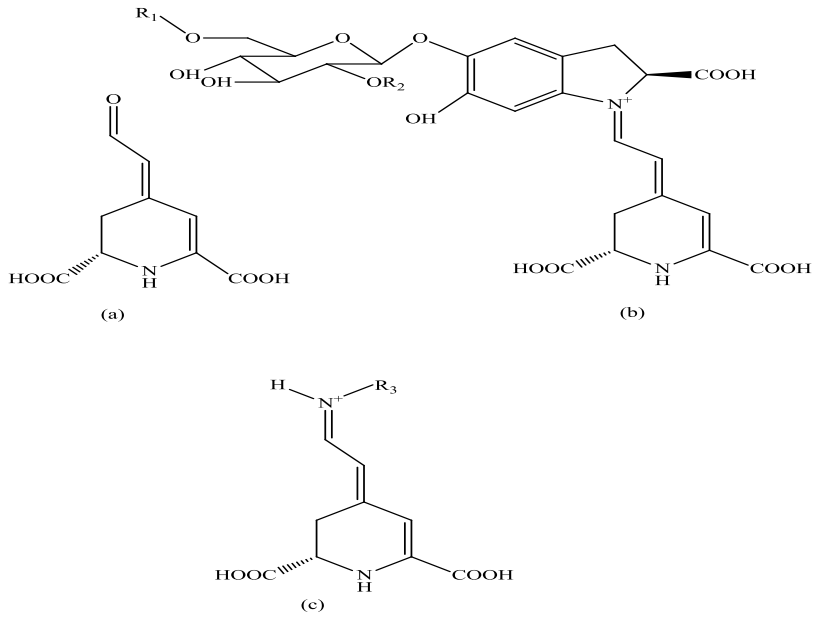

Figure 2. 9: General structures of: (a) betalamic acid, (b) betacyanin, and (c) betaxanthins.

The structural differences reflect in varying appearance of the betalain subgroups. Betanin is generally unstable when exposed to heat, light and oxygen, all of which have a degrading (and cumulative) effect on betanin. Generally, betanins are stable in slightly acidic environments (between pH 4.0 and 7.0). Betacyanins have visible spectra with maxima in the 535-550 nm ranges, and the exact absorption spectrum is dependent on pH and temperature.

2.4.3 Chlorophyll

Chlorophyll is a green pigment found in almost all plants, algae, and cyanobacteria. Chlorophyll is an extremely important biomolecule, critical in photosynthesis, which allows plants to obtain energy from light. Chlorophyll absorbs light most strongly in the blue portion of the electromagnetic spectrum, followed by the red portion.

Chlorophyll molecules are specifically arranged in and around photosystems that are embedded in the thylakoid membranes of chloroplasts. In these complexes,

chlorophyll serves two primary functions. The function of the vast majority of chlorophyll (up to several hundred molecules per photosystem) is to absorb light and transfer that light energy by resonance energy transfer to a specific chlorophyll pair in the reaction center of the photosystems.

The two currently accepted photosystem units are Photosystem II and Photosystem I, which have their own distinct reaction center chlorophylls, named P680 and P700, respectively [47]. These pigments are named after the wavelength (in nanometers) of their red-peak absorption maximum. The identity, function and spectral properties of the types of chlorophyll in each photosystem are distinct and determined by each other and the protein structure surrounding them. The function of the reaction center chlorophyll is to use the energy absorbed by and transferred to it from the other chlorophyll pigments in the photosystems to undergo a charge separation, a specific redox reaction in which the chlorophyll donates an electron into a series of molecular intermediates called an electron transport chain.

The basic structure of a chlorophyll molecule is a porphyrin ring, co-ordinated to a central atom. This is very similar in structure to the heme group found in hemoglobin, except that in heme the central atom is iron, whereas in chlorophyll it is magnesium. This is a stable ring-shaped molecule around which electrons are free to migrate. Because the electrons move freely, the ring has the potential to gain or lose electrons easily, and thus the potential to provide energized electrons to other molecules. This is the fundamental process by which chlorophyll "captures" the energy of sunlight.

There are actually two main types of chlorophyll, named *a* and *b*. They differ only slightly, in the composition of a side chain (in *a* it is $-CH_3$, in *b* it is CHO). Both of these two chlorophylls are very effective photoreceptors because they contain a

network of alternating single and double bonds, and the orbitals can delocalize stabilizing the structure. Such delocalized polyenes have very strong absorption bands in the visible regions of the spectrum, allowing the plant to absorb the energy from sunlight.

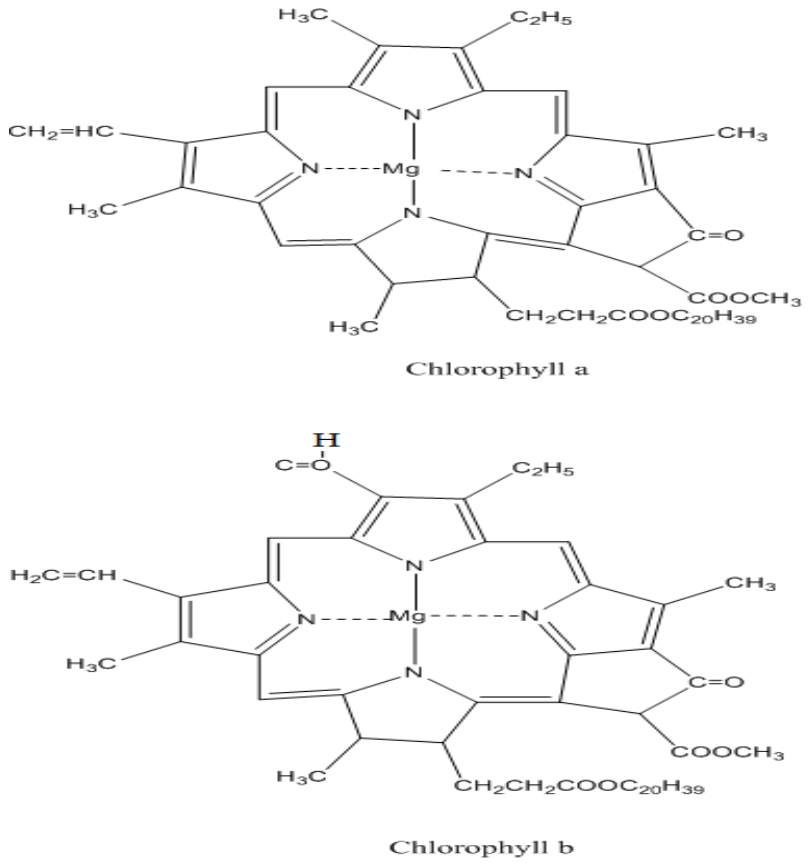

Figure 2. 10: Molecular structure of chlorophyll a and chlorophyll b.

The different side groups in the two chlorophylls adjust the absorption spectrum to slightly different wavelengths. Chlorophyll a absorbs well at a wavelength of about 400 - 450 nm and at 650 - 700 nm; chlorophyll b at 450 - 500 nm and at 600 - 650 nm, so that light that is not significantly absorbed by chlorophyll *a*, at, say, 460nm, will instead be captured by chlorophyll *b*, which absorbs strongly at that wavelength. Thus these two kinds of chlorophyll complement each other in absorbing sunlight.

There are two characteristic π–π* absorption regions, the weaker Q band at lower visible wavelengths (550 – 700 nm) and the intense Soret band in the near UV region (400 – 450 nm). Due to the strong light-harvesting capability of chlorophylls and their derivatives, they have been introduced into DSSCs as dye sensitizers [48].

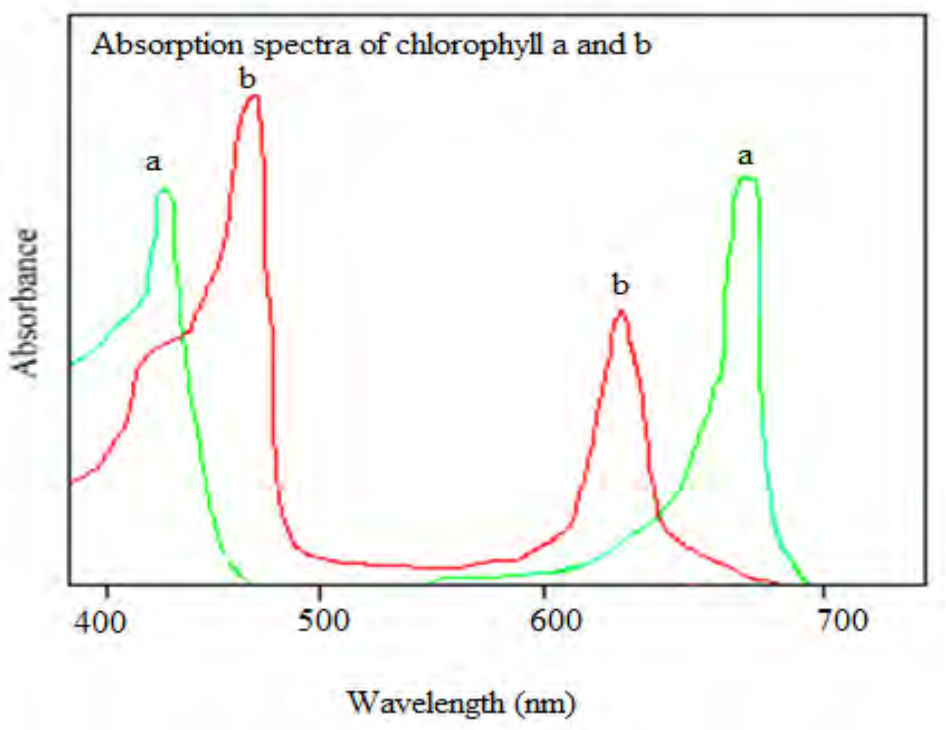

Figure 2. 11: The UV/visible adsorption spectrum for chlorophyll.

2.5 The Methods Used for The characterization of The DSSCs

A wide range of experimental methods are available with which to analyze various properties of the DSSCs. A complete description of these methods is, however, beyond the scope of this thesis, so only a summary of those, directly relevant to the coming discussion, will be presented.

2.5.1 Current-Voltage Characteristics

Current-voltage curve measurements are the most central way to characterize the photovoltaic (PV) device performance. The DSSC generates a current, I, and a voltage, V, when it is illuminated and connected to an outer circuit. If the resistance of the outer circuit is zero, the cell is short circuited (*SC*) and the current reaches a maximum value, I_{SC}, while the voltage is zero. Conversely, if the resistance of the outer circuit is infinite, the cell is open-circuited (OC) and the voltage reaches a maximum value, V_{OC}, while the current is zero.

The solar cell efficiency is determined by its current-voltage (I-V) characteristics under standard illumination conditions. A standard solar spectrum of air mass 1.5 (AM 1.5) with an intensity (the power of incident light) of 1000 W/m^2 also referred to as 1 sun, is used for solar cell characterization. The AM 1.5 spectrum corresponds to sunlight that has path through the atmosphere 1.5 times longer than when the sun is directly overhead [49]. The sunlight will be attenuated differently by the earth atmosphere dependent on the incident radiation angle. In the lab, the illumination conditions are provided by a calibrated lamp source.

The current-voltage characteristics are monitored under illumination by varying an external load from zero load (short-circuit condition) to infinite load (open-circuit condition). A typical current-voltage characteristic of a solar cell is illustrated in Figure 2.11.

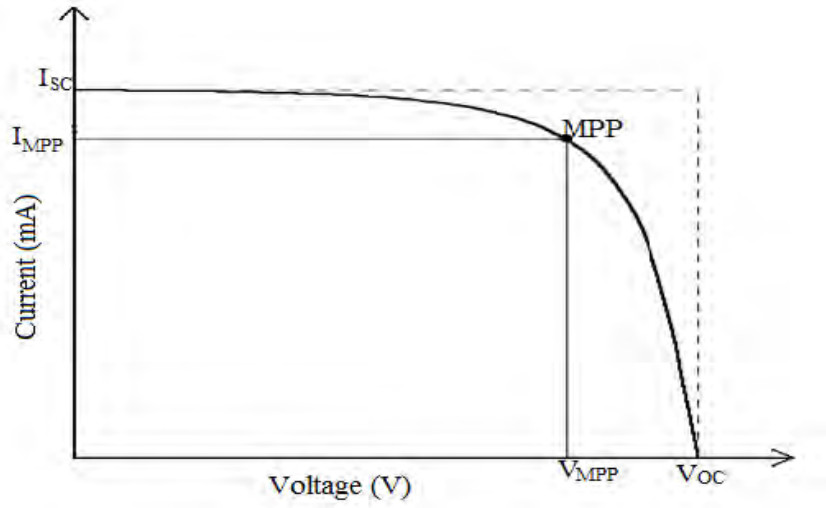

Figure 2. 12: Current - voltage characteristics of a DSSC illustrating short-circuit current (I_{SC}), open-circuit voltage (V_{OC}), current at maximum power point (I_{MPP}) and voltage at maximum power point (V_{MPP}).

The maximum power generated is when the product of the current and voltage is maximum, since the electrical power is given by current (I) times voltage (V), i.e P = IV. The short-circuit current and the open-circuit voltage are the maximum current and voltage, respectively from a solar cell. However, at both of these operating points, the power from the solar cell is zero. The "fill factor", more commonly known by its abbreviation "FF", is a parameter which, in conjunction with V_{OC} and I_{SC}, determines the maximum power from a solar cell. The FF is defined as the ratio of actual maximum power from the solar cell to the product of V_{OC} and I_{SC}. The fill-factor (FF) of the cell can be calculated from Equation 6.

$$FF = \frac{I_{MPP} \cdot V_{MPP}}{I_{SC} \cdot V_{OC}} \qquad (6)$$

Graphically, the FF is a measure of the "squareness" of the solar cell and is also the area of the largest rectangle which will fit in the current - voltage curve. For example,

resistive losses in the cell show directly from the shape of the current - voltage (I - V) curve, making it “flatter” and decreasing the fill factor. The cell efficiency (η) can be calculated using the fill factor, or directly from the I_{MPP} and V_{MPP} using Equation 7.

$$\eta = \frac{P_{out}}{P_{in}} = \frac{I_{SC} \cdot V_{OC} \cdot FF}{P_{in} \cdot A} \tag{7}$$

where P_{in} is the power of incident light on the cell and A is the photoactive area of the cell, i.e. in the case of the DSSC, the area of the dye-sensitized TiO_2 film.

The current - voltage characteristics can also be monitored at dark conditions. The difference between light and dark measurement is that in light, the recombination current (also called dark current) is counter balanced by the photocurrent, reaching at open circuit conditions when both currents are equal and no net current is longer extracted. When a load is present, a potential difference develops between the terminals of the cell. This potential difference generates a current which acts in the opposite direction to the photocurrent, and the current is reduced from its short circuit value. This reverse current is usually called the dark current which flows across the device under bias in the dark. At voltages higher than open circuit conditions (V > Voc) the net current is dominated by the dark current and is going in the opposite direction. At $V > V_{OC}$ the device consumes power and at $V < 0$, the illuminated device acts as a photodetector, consuming power to generate a photocurrent which is light dependent but bias independent.

2.5.2 Incident Photon to Current Conversion Efficiency

Incident photon to current-conversion efficiency (IPCE) reveals how efficiently light of a specific wavelength is converted to current, as expressed in Equation 8.

$$IPCE = \frac{1240(eV.nm) \cdot I_{SC}(mAcm^{-2})}{\lambda(nm) \cdot P_{in}(mWcm^{-2})} \quad (8)$$

Where λ is the wavelength of the incident light, and P_{in} is the intensity of the incident light.

Depending of the dye molecule and its spectral properties when attached to the TiO_2, IPCE varies with respect to wavelength.

2.6 Objectives

2.6.1 General Objective:

- To screen natural dyes and construct dye sensitized solar cells based on natural dyes extracted from natural flowers.

2.6.2 Specific Objectives:

- To screen the natural dyes from natural flowers such as *Amaranthus caudatus*, *Bougainvillea spectabilis*, *Delonix regia, Nerium oleander* and *Spathodea campanulata*.
- To construct natural dye- sensitized photoelectrochemical solar cells.
- To characterize the device constructed using standard optical and photoelectrical techniques.

3. EXPERIMENTAL

3.1 Preparation of Natural Dye Sensitizers

Enough amounts of the natural flowers such as *Amaranthus caudatus* (colour of the flower: deep red), *Bougainvillea spectabilis* (colour of the flower: deep red), *Delonix regia* (colour of the flower: red), *Nerium oleander* (colour of the flower: rose) and *Spathodea campanulata* (colour of the flower: red) were collected from Arba Minch Zone, South Nationalities Peoples Region, 551 kilometers south of Addis Ababa. After collection, the plant materials were identified by a taxonomist and dried under shade area for 30 days and crushed to powder for extraction.

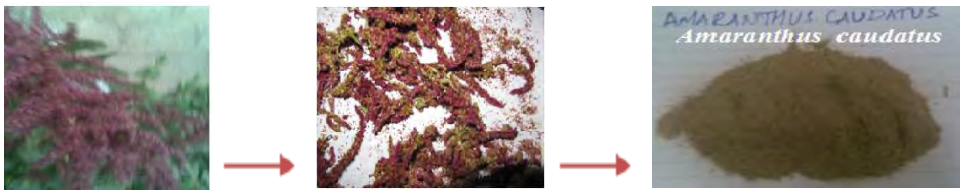

(a)

(b)

(c)

(d)

(e)

Figure 3.1: Plant materials used in this study (a) *Amaranthus caudatus* and (b) *Bougainvillea spectabilis* (c) *Delonix regia* (d) *Nerium oleander* and (e) *Spathodea campanulata*.

Amaranthus caudatus powder of 3 g and *Bougainvillea spectabilis* powder of 3 g were separately extracted in 200 ml of ethanol and 200 ml of 0.1 M HCl-water at room temperature. A mixed dye was prepared by mixing separately ethanol extracted *Amaranthus caudatus* and *Bougainvllea spectabilis* solution to 0.1 M HCl-water extracted solution at a ratio of 1:1 by volume respectively. The powders of rest three plant materials of 3 g were separately extracted in 200 ml of 0.1 M HCl-water at room temperature. The glass containers were covered with aluminium foils to prevent damage from light exposure and were left to shake for one day. Thereafter the solid residues were filtered out to obtain clear dye solutions.

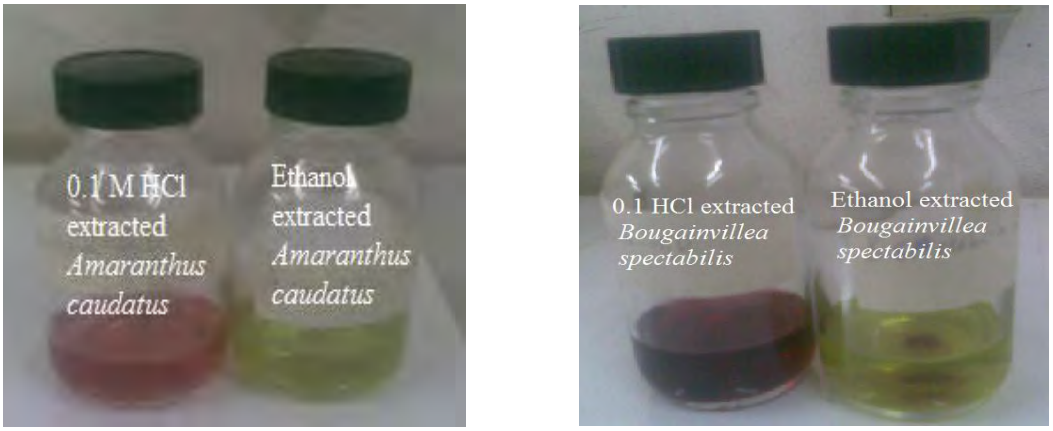

(a) (b)

Figure 3.2: Extracts of plant materials (a) *Amaranthus caudatus* and (b) *Bougainvillea spectabilis* in different solvent.

3.2 Preparation of TiO_2 Electrode (Photoanode)

ITO conductive glass sheets (2.5 cm × 1.5 cm) were first cleaned with acetone (Aldrich), 2-propanol (Riedel-de Haen) and ethanol (Fluka) for 30 minutes in each step using ultrasonic bath.

Preparation of mesoporous titanium dioxide (TiO_2) paste was done with the method described elsewhere [6]. The preparation of nanocrystalline films employed commercial titanium dioxide nanopowder (P25, Degussa AG, Germany, a mixture of about 30% rutile and 70% anatase). In order to break the aggregates into separate particles, the powder (3 g) was ground in a porcelain mortar with a small amount of water (1 mL) containing acetic acid (0.1 mL) to prevent reaggregation of the particles. After the powder had been dispersed by the high shear forces in the viscous paste, it was diluted by slow addition of water (4 mL) under continued grinding. Finally, a detergent (0.05 mL Triton X-100, Aldrich) was added to facilitate the spreading of the colloid on the substrate. The ITO was covered on two parallel edges with adhesive tape to control the thickness of the TiO_2 film and to provide non-coated areas for electrical contact. The colloid was applied to one of the free edges of the conducting glass and distributed with a glass rod sliding over the tape-covered edges as shown Figure 3.3. After air drying, the electrode was fired for 30 min at 450^0C in a furnace (Carbolite Model ELF 11/14B).

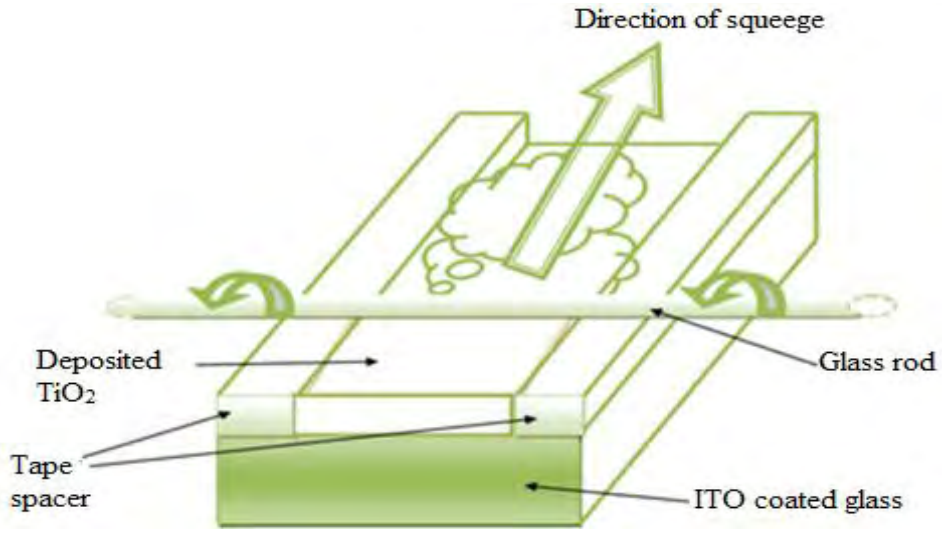

Figure 3.3: TiO_2 film preparation procedure.

Coating of the TiO_2 surface with dye was carried out by soaking the film for overnight in the dyes extracted. After completion of the dye adsorption, the electrode was withdrawn from the solution under a stream of dry air. It was stored in dry ethanol or immediately wetted with redox electrolyte solution for testing.

3.3 Preparation of Counter Electrode

The PEDOT film on ITO for the counter electrode was formed by electrochemical polymerization of EDOT (Aldrich), in a three electrode one-compartment electrochemical cell.

The electrochemical cell consisted of a pre-cleaned ITO-coated glass working electrode, platinum foil counter electrode and quasi-Ag/AgCl reference electrode. The solution used for the polymerization contained 0.2 M EDOT and 0.1 M $(C_2H_5)_4NBF_4$ (Aldrich) in acetonitrile (Sigma-Aldrich). The monomer was used as received. The polymerization was carried out potentiostatically at +1.8 V for 2 seconds. At this potential, the electrode surface becomes covered with blue-doped PEDOT film. The cell was then rinsed with acetonitrile and dried in air.

3.4 Preparation of Electrolyte

The polymer gel electrolyte was prepared by the following process [50]. 0.9 M of EMIM-I was added into acetonitrile (Aldrich) under stirring to form a homogeneous liquid electrolyte. In order to obtain a better conductivity, 0.5 M of sodium iodide (BDH) was dissolved in the above homogeneous liquid electrolyte, and then 0.12 M iodine and 35% (w/w) of PVP (Aldrich) were added. Then, the resulting mixture was heated at 70 – 80^0C under vigorous stirring to dissolve the PVP polymer, followed by cooling down to room temperature to form a gel state electrolyte. Finally, the gel

electrolyte was deposited in the form of thin film on top of the dye coated TiO_2 electrode. The PEC solar cell was completed by pressing against PEDOT-coated ITO glass counter electrode. The PEC solar cell was then mounted in a sample holder inside a metal box with an area of 1 cm^2 opening to allow light from the source. All experiments were carried out at ambient temperature.

3.5 Assembling of the Complete Photoelectrochemical Cells (PECs)

The photoelectrode and the counter electrode were overlappingly placed in a holder so that the titanium dioxide covered area of the photoelectrode was the only part of the photoelectrode that was in contact with the counter electrode. The non-titanium dioxide covered area of the photoelectrode and the non-overlapping edge of the counter electrode were attached to the measuring equipment by means of cords and crocodile clips.

3.6 Measurement

The photoelectrochemical measurements of the cell were performed using a computer controlled CHI630A Electrochemical Analyzer. A 150-W Xenon lamp regulated by an Oriel power supply (Model 68830) was used to illuminate the PEC. A grating monochromator (Model 77250) placed into the light path was used to select a wavelength between 300 and 800 nm. The measured photocurrent spectra were corrected for the spectral response of the lamp and the monochromator by normalization to the response of a calibrated silicon photodiode (Hamamatsu, Model S1336-8BK) whose sensitivity spectrum was known. No correction was made for the reflection from the surface of the sample. The white light intensity was measured in the position of the sample cell with Gigahertz-Optik $X1_1$ Optometer. The intensity of

the incident light was 100 m Wcm^{-2}. The absorption spectra of dye solutions were recorded using GENESYS 2PC UV–Vis spectrometer.

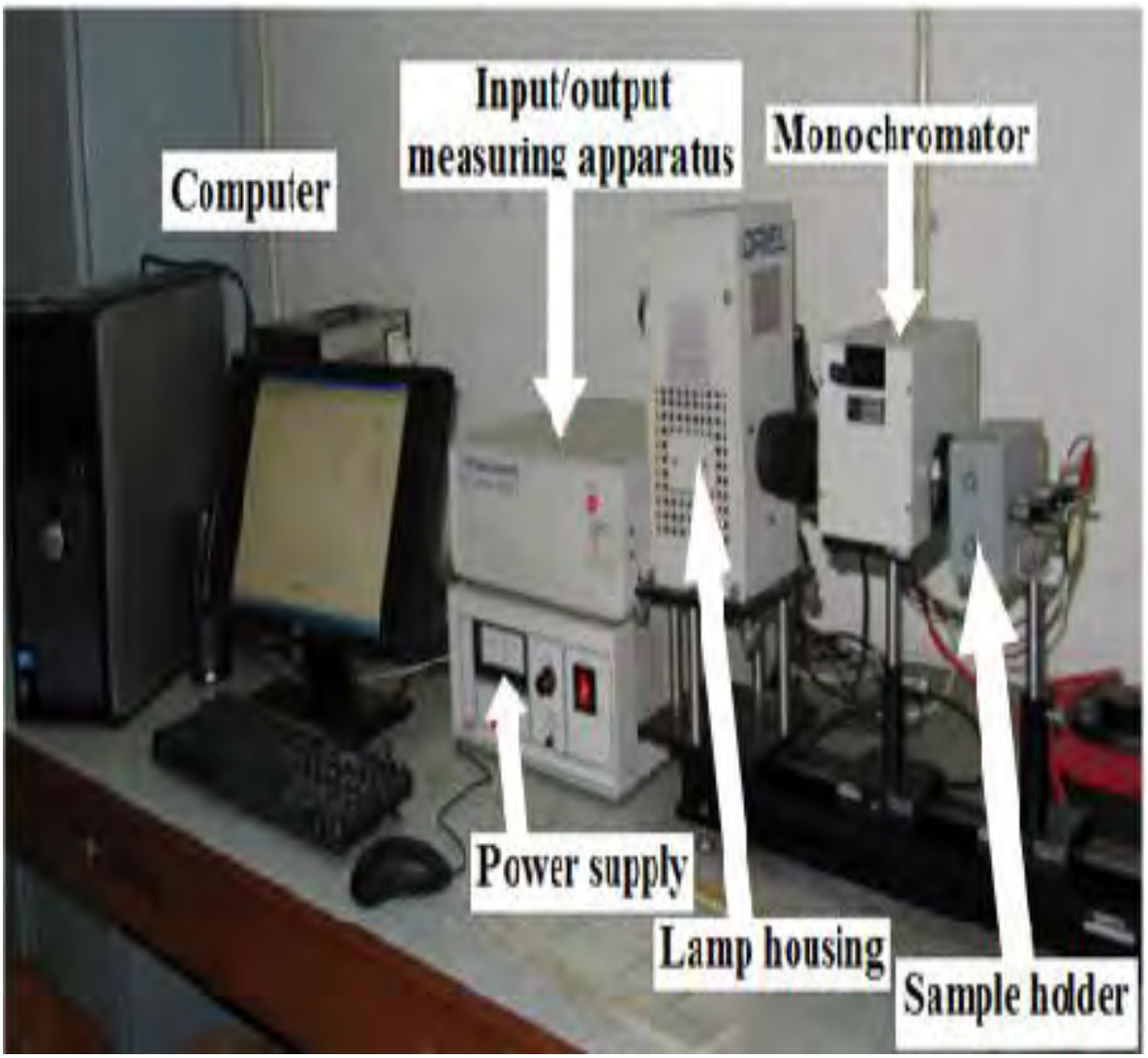

Figure 3. 4: General experimental set-up for photoelectrochemical measurements.

4. RESULTS AND DISCUSSION

4.1. Absorption Spectra of Natural Dyes

We attempted to use 5 kinds of colorful natural dyes as sensitizers for DSSCs. Figure 4.1 and 4.2 shows the UV-vis absorption spectra for the ethanol, 0.1 M HCl-water, and mixed extracts of 0.1 M HCl-water and ethanol solutions of *Amaranthus caudatus* and *Bougainvillea spectabilis,* respectively. Figure 4.1and 4.2 exhibits that the ethanol extracts of *Amaranthus caudatus* and *Bougainvillea spectabilis*, whose colors are green, reach a maximum absorption peaks of 665 nm, 413 nm for *Amaranthus caudatus* and *Bougainvillea spectabilis*. The main component of these two extracts is chlorophyll.

Figure 4.1 and 4.2 also demonstrates that the 0.1 M HCl- water extracts of *Amaranthus caudatus* and *Bougainvillea spectabilis*, whose colors are red, *Amaranthus caudatus* extract displayed an intense absorption in the 500 - 600 nm region due to of the red-purple betacynines and *Bougainvillea spctabilis* extract displayed an intense absorption in the 400 – 600 nm region due to the mixed contributions of the yellow-orange betaxanthins (480 nm) and of the red-purple betacyanines (540 nm) [51]. Furthermore, the absorption peaks of mixed dyes of *Amaranthus caudatus* extracts and *Bougainvillea spctabilis* extracts are displayed in Figure 4.1 and 4.2. As displayed in Figure 4.1 and 4.2, the absorption peaks of the mixed dyes are in the visible light range about 670 nm, and 536 nm for dyes mixed extract of *Amaranthus caudatus* and about 668 nm, 536 nm, 479 nm, 446 nm, and 416 nm for dyes mixed extract of *Bougainvillea spctabilis*. The light absorption spectrum of the mixed extract contained peaks corresponding to the contributions from the individual extracts.

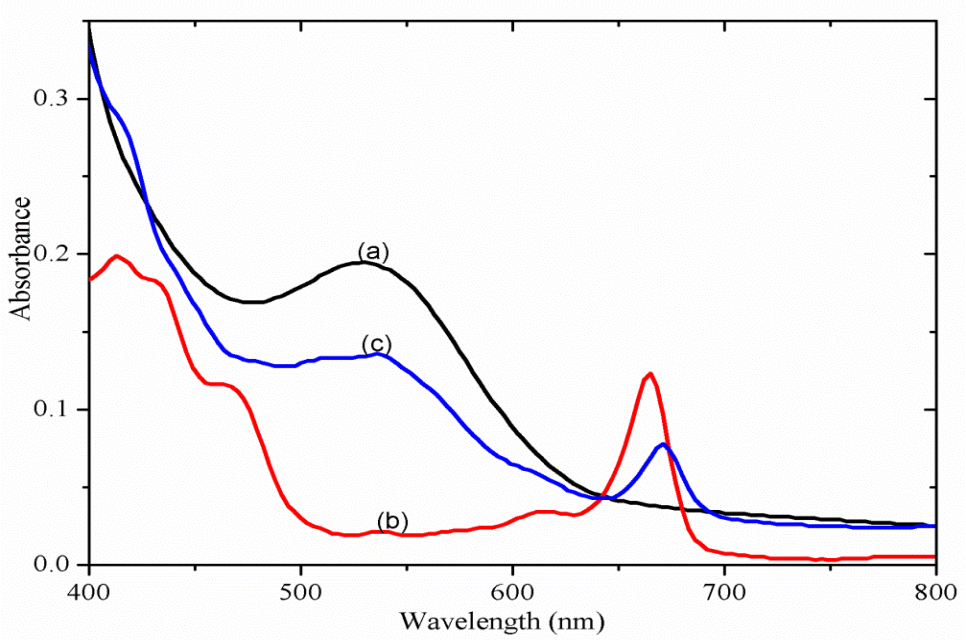

Figure 4. 1: UV-vis absorption spectra of dye solutions of: (a) 0.1 M HCl-water extracted *Amaranthus caudatus* extract, (b) ethanol extracted *Amaranthus caudatus* extract and (c) mixture of dyes extracted in 0.1 M HCl-water and ethanol.

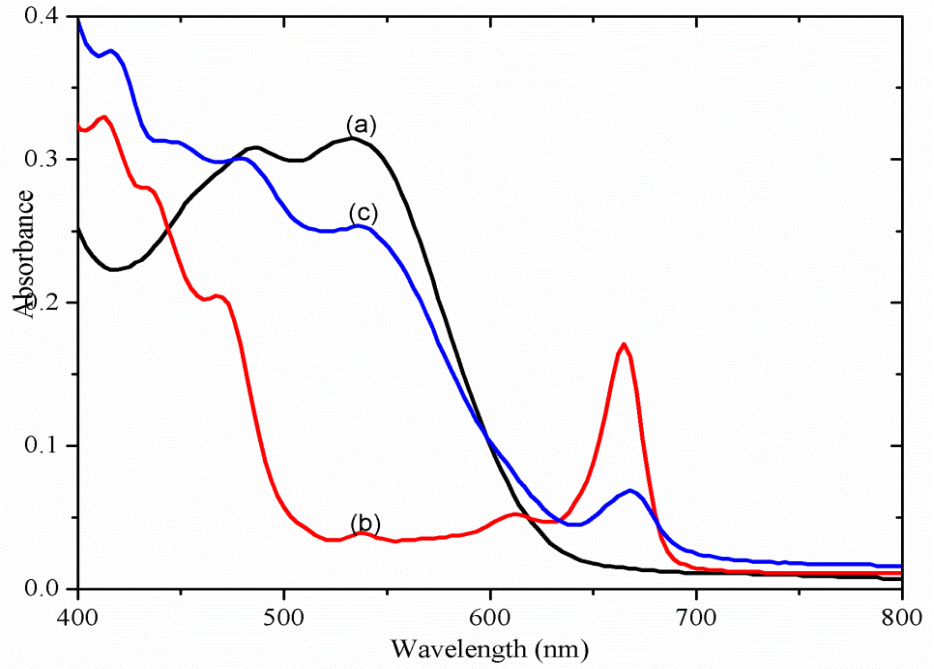

Figure 4. 2: UV-vis absorption spectra of dye solutions of: (a) 0.1 M HCl-water extracted *Bougainvillea spctabilis* extract, (b) ethanol extracted *Bougainvillea spctabilis* extract and (c) mixture of dyes extracted in 0.1 M HCl-water and ethanol.

Figure 4.3 shows the UV-Vis absorption spectra of *Delonix regia*, *Nerium oleander* and *Spathodea companulata* in 0.1 M HCl -water solution. From Figure 4.3, it can be seen that there is an absorbent peak at about 516 nm for extract of *Delonix regia.* This absorption ascribes to their identical components, namely, anthocyanins, a group of natural phenolic compounds [52]. Anthocyanin is the core component of some natural dyes and is often found in the fruits, flowers, and leaves of plants. Because anthocyanin shows color in the range of visible light from red to blue, it is predicted to become a highly efficient sensitizer for wide band gap semiconductors [53]. The Nerium *oleander* and *Spathodea companulata* in 0.1 M HCl-water solution do not show obvious maximum absorption peaks in the visible light region as observed in Figure 4.3.

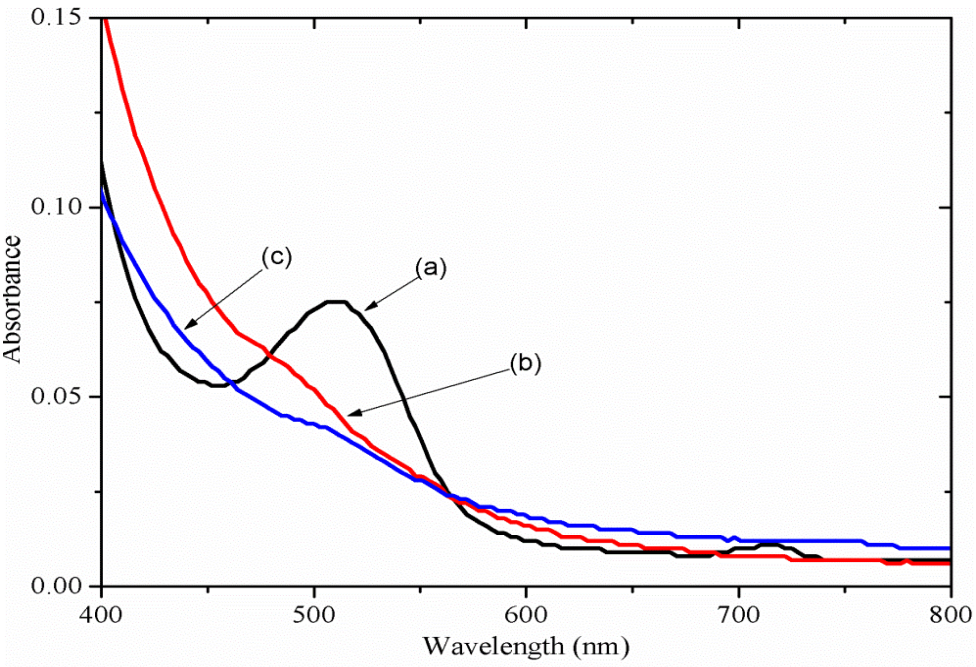

Figure 4. 3: UV-vis absorption spectra of dye solutions of: (a) *Delonix regia*, (b) *Nerium oleander* and (c) *Spathodea companulata* extracted with 0.1 M HCl-water.

4.2. Photoelectrochemical Properties of DSSCs Sensitized with Natural Dyes

Photovoltaic tests of DSSCs using these natural dyes as sensitizers were performed by measuring the current density – voltage (J – V) curves under irradiation with white light (100 $mWcm^{-2}$). The performance of natural dyes as sensitizers in DSSCs was evaluated by short circuit current density (J_{SC}), open circuit voltage (V_{OC}), fill factor (FF), and energy conversion efficiency (η). The photoelectrochemical parameters of the DSSCs sensitized with natural dyes are listed in Table 4.1. It presents the performance of the DSSCs in terms of short-circuit photocurrent density (J_{SC}), open-circuit voltage (V_{OC}), fill factor (FF) and energy conversion efficiency (η) compared to those of other extracts not in this work.

The typical current density - voltage (J – V) curves of the DSSCs using the sensitizers extracted from *Amaranthus caudatus*, *Bougainvillea spectabilis*, *Delonix regia*, *Nerium oleander*, and *Spathodea companulata* are shown in Figure 4.4, 4.5 and 4.6., respectively. As shown in Table 4.1, Figure 4.4, 4.5 and 4.6, the fill factors of these DSSCs are mostly higher than 50%. The open circuit voltage (V_{OC}) varies from 0.45 to 0.55 V, and the short circuit photocurrent density (J_{SC}) changes from 0.013 to 1.82 $mAcm^{-2}$. Specifically, a high open circuit voltage (V_{OC} = 0.55 V) and short circuit photocurrent density (J_{SC} = 1.82 $mAcm^{-2}$) were obtained from the DSSC sensitized by the *Amaranthus caudatus* extracted extract with ethanol; the efficiency of the DSSC reached 0.61%. These data are significantly higher than those of the DSSCs sensitized by other natural dyes in this work and showed a comparable performance to the DSSCs prepared from other natural dyes done by other groups [54] (Table 4.1). This is due to a broader range of the light absorption of the extract adsorbed on TiO_2, and the higher interaction between TiO_2 and chlorophyll in the *Amaranthus caudatus*

extract leads to a better charge transfer. Moreover, chlorophyll in the *Amaranthus caudatus* extract may has the shortest distance between the dye skeleton and the point connected to TiO_2 surface compared to that of other extracts in this work. This could facilitate an electron transfer from chlorophyll in the *Amaranthus caudatus* extract to the TiO_2 surface and could be accounted for a better performance of *Amaranthus caudatus* extract sensitization [55]. Chlorophyll plays an important role in plant photosynthesis; the DSSCs using chlorophyll derivatives as sensitizers obtained a relatively high conversion efficiency [56, 57]. This is because there are available bonds between the dye and TiO_2 molecules through which electrons can transport from the excited dye molecules to the TiO_2 film [58]. This result indicates that the interaction between the sensitizer and the TiO_2 film is significant in enhancing the energy conversion efficiency of DSSCs.

The photovoltaic properties of the DSSCs sensitized by the dyes extracted from *Amaranthus caudatus* and *Bougainvillea spectabilis* with various solvents were studied by measuring current density - voltage (J – V) curves, and the corresponding photoelectrochemical parameters are listed in Table 4.1. As observed, the efficiencies of the DSSCs using ethanol extracted extracts and 0.1 M HCl - water extracted extracts as sensitizers are 0.61%, 0.033% for *Amaranthus caudatus* and 0.325%, 0.018% for *Bougainvillea spectabilis* respectively. The photoelectrochemical performances of DSSCs using the dye mixed solutions were also investigated. The efficiencies of dye mixed solutions are 0.114% for *Amaranthus caudatus* and 0.164% for *Bougainvillea spectabilis,* respectively. The efficiency of DSSC using dye mixed solution as sensitizer is much lower than the sum of the efficiencies of the DSSCs sensitized with ethanol extracts and 0.1 M HCl -water extracts. This result indicates that the mixed extract adsorbed on TiO_2 does not show synergistic photosensitization

compared with individual extracts, which is in accordance with the results reported by Wongcharee et al. [59]. However, this is rather different from the result reported by Kumara and co-workers [60], in which a DSSC fabricated using chlorophyll and shisonin dyes showed synergistic effect of both dyes. We hypothesize two possible reasons for this phenomenon in which the mixed extract of *Amaranthus caudatus* and *Bougainvillea spectabilis* did not show synergistic photosensitization. First, although the DSSC sensitized with the mixed extracts of *Amaranthus caudatus* and *Bougainvillea spectabilis* utilize the light of several spectral regions, the coadsorption suppresses electron injection possibly due to the increase in concentration quenching. Second, the strong steric hindrance of basic molecular structures for the main components of the extracts of *Amaranthus caudatus* and *Bougainvillea spectabilis* with various solvents prevents the dye molecules from effectively arraying on the TiO_2 film. Hence, this leads to a deficiency of electron transfer from dye molecules to conducting band of TiO_2.

The photovoltaic properties of the dye-sensitized solar cells (DSSCs) sensitized by the dyes extracted from *Delonix regia*, *Nerium oleander* and *Spathodea companulata* with 0.1 M HCl-water solvent were studied by measuring current density – voltage (J – V) curves, and the corresponding photoelectrochemical parameters are listed in Table 4.1. As noticed, the efficiencies of the DSSCs using 0.1 M HCl-water extracted extracts as sensitizers are 0.03% for *Delonix regia*, 0.013% for *Nerium oleander* and 0.003% for *Spathodea companulata*. In the case of *Delonix regia* identical components is anthocyanin. Carbonyl and hydroxyl groups present in the anthocyanin molecule can be bound to the surface of a porous TiO_2 film. This makes electron transfer from the anthocyanin molecule to the conduction band of TiO_2, which favors the photoelectric conversion effect. However, the DSSCs sensitized by

natural dyes mainly composed of anthocyanin in this work, such as *Delonix regia*, did not offer high conversion efficiencies. This is because there are no available bonds between the dye and TiO_2 molecules through which electrons can transport from the excited dye molecules to the TiO_2 film [58].

Table 4. 1: Photoelectrochemical parameters of the DSSCs sensitized by: (a) ethanol extracted natural dyes, (b) 0.1 M HCl- water extracted natural dyes and (c) mixture of dyes extracted in 0.1 M HCl- water and ethanol (dye mixed solution).

Natural dye	J_{SC} ($mAcm^{-2}$)	V_{OC} (V)	FF (%)	η (%)	Reference
Amaranthus caudatus[a]	1.82	0.55	61	0.61	
Amaranthus caudatus[b]	0.102	0.53	61	0.033	
Amaranthus caudatus[c]	0.44	0.45	58	0.114	
Bougainvillea spectabilis[a]	1.11	0.5	58.6	0.325	
Bougainvillea spectabilis[b]	0.081	0.45	48.3	0.018	
Bougainvillea spectabilis[c]	0.648	0.47	54	0.164	
Delonix regia[b]	0.114	0.47	57.9	0.031	
Nerium oleander[b]	0.046	0.5	57.5	0.013	
Spathodea companulata[b]	0.013	0.46	44	0.003	
Begonia[a]	0.63	0.537	72.2	0.24	
Bauhinia tree[a]	0.96	0.572	66	0.36	
China loropetal[a]	0.84	0.518	62.6	0.27	
Tangerine[a]	0.74	0.592	63.1	0.28	[54]
Rhododendron[a]	1.61	0.585	60.9	0.57	
Lithospermum[a]	0.14	0.337	58.5	0.03	
Mangosteen pericarp[a]	2.69	0.686	63.3	1.17	
Fructus lycii[a]	0.53	0.689	46.6	0.17	

[a]Ethanol extracted natural dye, [b]0.1 M HCl extracted natural dye, and [c]Mixture of natural dyes extracted from ethanol and 0.1M HCl-water.

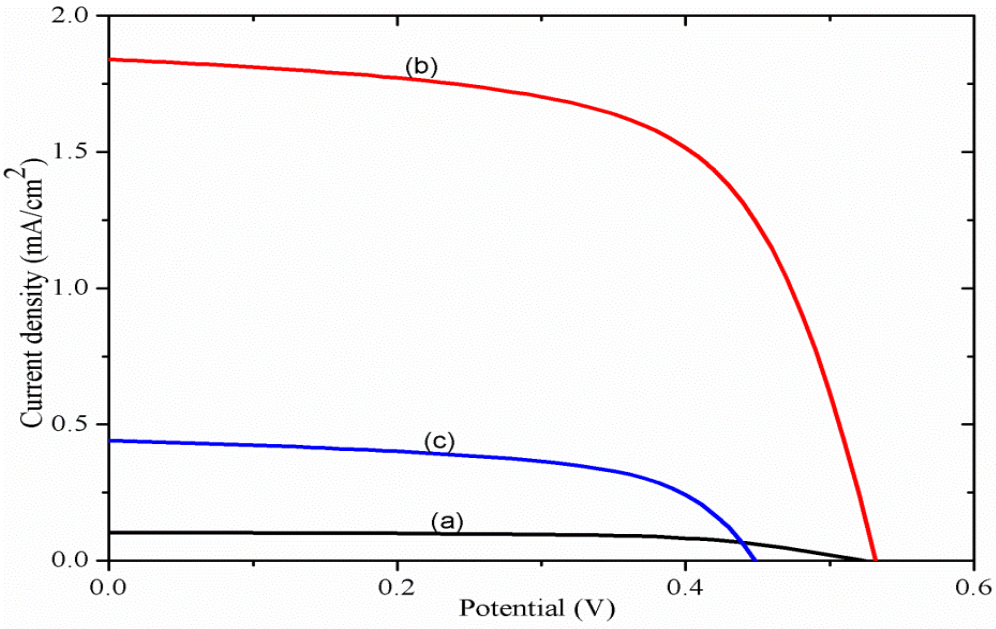

Figure 4. 4: Current density–voltage curves for DSSCs sensitized by the extract of *Amaranthus caudatus* extracted from: (a) 0.1 M HCl–water, (b) ethanol and (c) mixture of dyes extracted in 0.1 M HCl-water and ethanol.

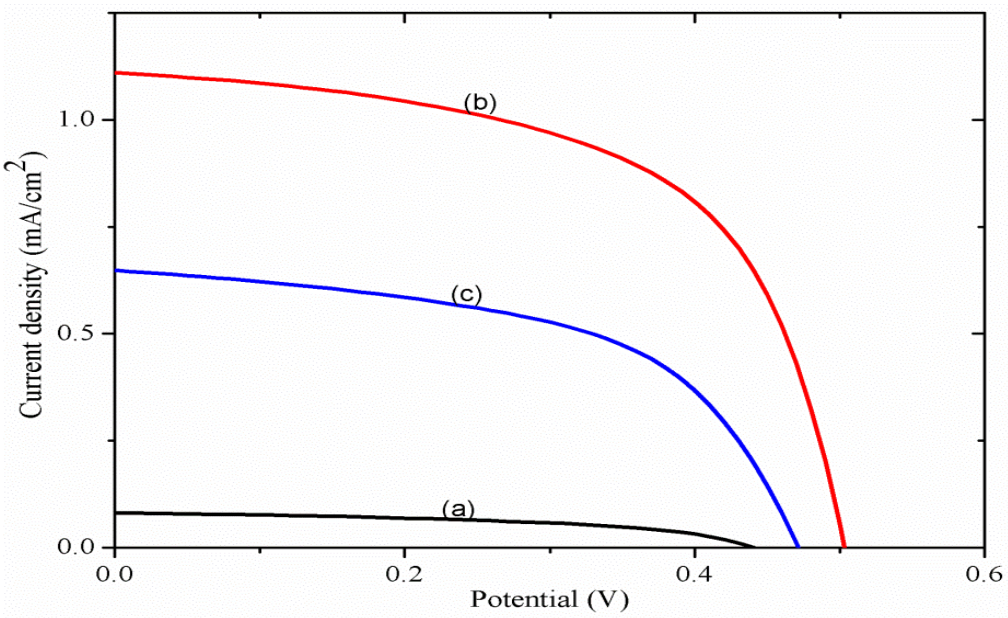

Figure 4. 5: Current density–voltage curves for DSSCs sensitized by the extract of *Bougainvillea spectabilis* extracted from: (a) 0.1 M HCl–water, (b) ethanol and (c) mixture of dyes extracted in 0.1 M HCl –water and ethanol.

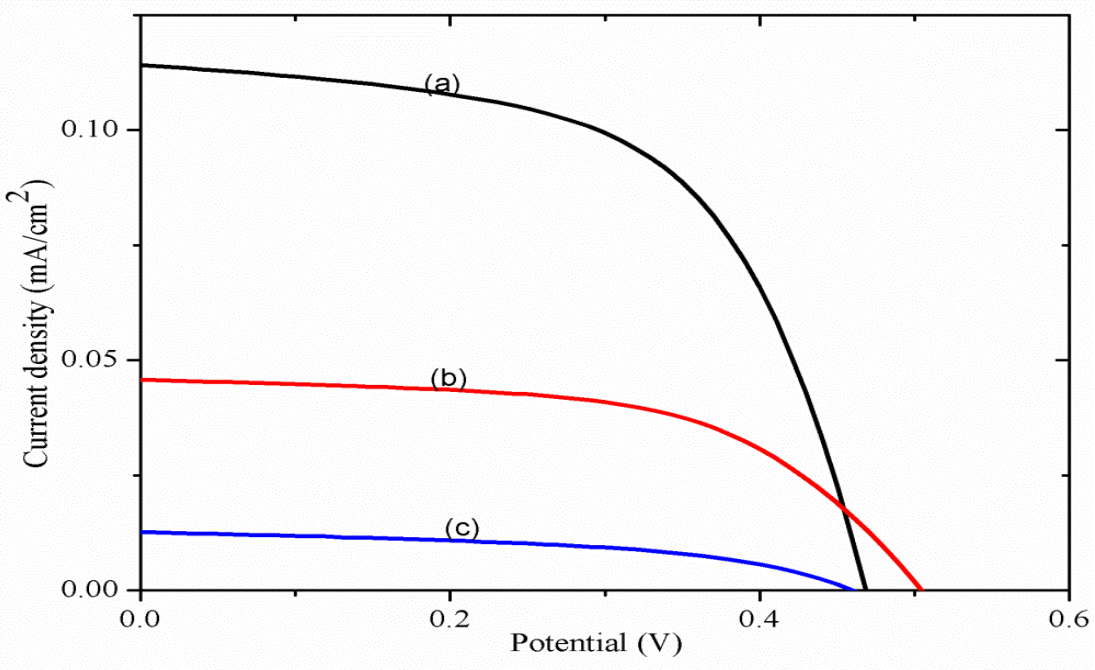

Figure 4. 6: Current density–voltage curves for DSSCs sensitized by: (a) the extract of *Delonix regia*, (b) the extract of *Nerium oleanders* and (c) the extract of *Spathodea companulata* extracted from 0.1 M HCl–water.

4.3 Incident Monochromatic Photon to Current Conversion Efficiency

The IPCE of DSSCs with TiO_2 photoelectrode was determined using Equation (8). Figure 4.7 – 4.9 show the action spectra for the DSSC sensitized with natural pigments. From Figure 4.7 in the wavelength range 300 – 800 nm, the IPCE plot exhibits a maximum of 52% at 430 nm with ethanol extract for *Amaranthus caudatus* pigment-sensitized PEC solar cell. The IPCE peaks of 0.1 M HCl-water extract and mixed dye extract for *Amaranthus caudatus* pigment-sensitized PEC solar cells occurring at 350 nm with 6.8% and 320 nm with 43.5%, respectively, are due to direct light harvesting by bare TiO_2 semiconductor [35]. However, the action spectra at wavelengths 400 – 600 nm originates from the dye molecules adsorbed on the TiO_2

surface. From Figure 4.8 in the wavelength range 300 – 800 nm, the IPCE plot shows a maximum of 27.7% at 410 nm with ethanol extract for *Bougainvillea spctabilis* pigment- sensitized PEC solar cell. The IPCE peaks of 0.1 M HCl –water extract and a mixed dye extract for *Bougainvillea spctabilis* pigment- sensitized PEC solar cells occurring at 345 nm with 5.8% and 330 nm with 16.7%, respectively, are due to direct light harvesting by bare TiO_2 semiconductor [35]. However, the action spectra at wavelengths 400 – 600 nm originates from the dye molecules adsorbed on the TiO_2 surface. From Figure 4.9 in the wavelength range 300 – 800 nm, the IPCE plot exhibits a maximum of 5.1% at 340 nm for *Delonix regia* pigment- sensitized PEC solar cell and of 4.7% at 330 nm for *Nerium oleander* pigment- sensitized PEC solar cell, which is the action spectral response of the bare TiO_2 semiconductor [35], but beyond 400 nm there is still action spectra response which is contributed by sensitization of extracts. For *Amaranthus caudatus, Bougainvillea spctabilis,* and *Delonix regia* pigment- sensitized PEC solar cells it was observed that the spectra response shows a blue-shift due to the electronic coupling between dye and TiO_2. The results from the IPCE data are consistent with the results from the J−V curves. The IPCE of the DSSC depends on the incident light harvesting and light scattering [61]. The former is due to the surface area of TiO_2 and the dye adsorbed amount whereas the latter is related to the morphology of TiO_2.

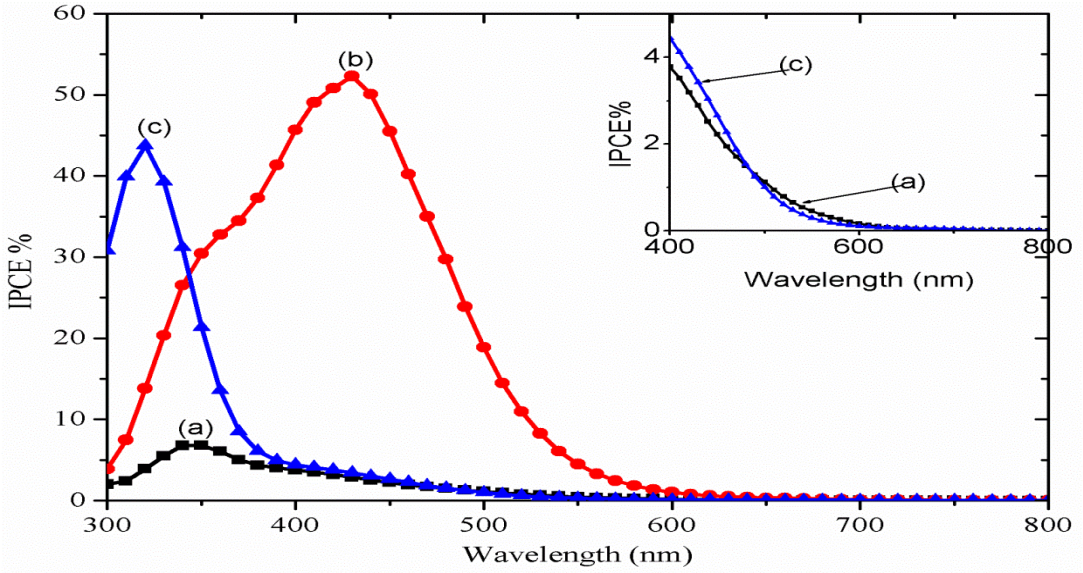

Figure 4. 7: IPCE curves for DSSCs sensitized by the extract of *Amaranthus caudatus* extracted from: (a) 0.1 M HCl–water, (b) ethanol and (c) mixture of dyes extracted in 0.1 M HCl and ethanol. Inset represents the IPCE of curves (a) and (c) in the wavelength range from 400 – 600 nm.

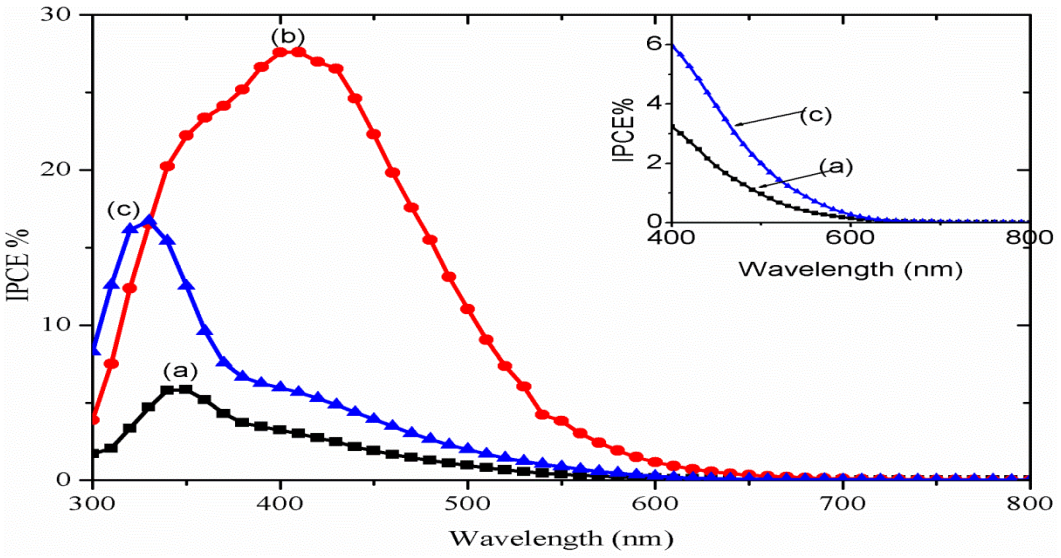

Figure 4. 8: IPCE curves for DSSCs sensitized by the extract of *Bougainvillea spectabilis* extracted from: (a) 0.1MHCl–water, (b) ethanol and (c) mixture of dyes extracted in 0.1 M HCl-water and ethanol. Inset represents the IPCE of curves (a) and (c) in the wavelength range from 400 – 600 nm.

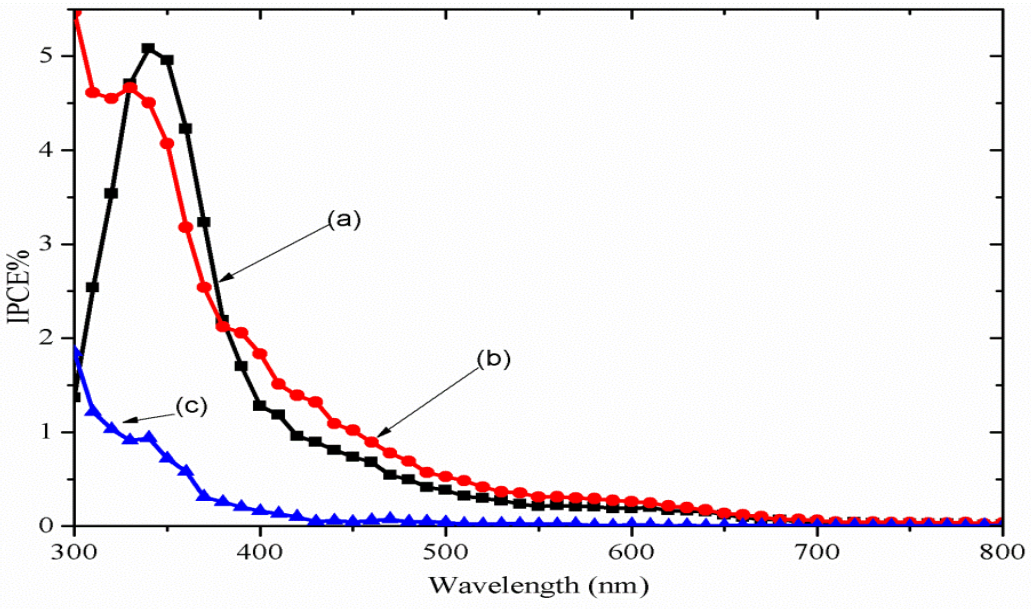

Figure 4. 9: IPCE curves for DSSCs sensitized by: (a) the extract of *Delonix regia*, (b) the extract of *Nerium oleanders*, and (c) the extract of *Spathodea companulata* extracted from 0.1 M HCl–water.

5. CONCLUSIONS

Five dyes obtained from natural flowers were used as sensitizers in DSSCs. The dyes extracted from these materials contained chlorophyll, betalains, anthocyanins, etc. The photoelectrochemical performance of the DSSCs based on these dyes showed that the open circuit voltage (V_{OC}) ranged from 0.45 – 0.55 V, and short circuit photocurrent density (J_{SC}) was in the range of 0.013 – 1.82 $mAcm^{-2}$. The DSSC sensitized by *Amaranthus caudatus* pigment extracted with ethanol offered the highest conversion efficiency of 0.61% among the five extracts. This is due to the better charge transfer between the *Amaranthus caudatus* dye molecule and the TiO_2 surface which is related to a dye structure. The photoelectrochemical performance for the extracts of *Amaranthus caudatus* and *Bougainvllea spectabilis* with different solvents indicated that the extracting solvent has an effect on the efficiency of DSSCs. DSSC using ethanol as a solvent shows a higher efficiency than that of using 0.1 M HCl water, reported at 0.61%, 0.033%, 0.325% and 0.018%, respectively, for *Amaranthus caudatus* and *Bougainvllea spectabilis.* Therefore, the ethanol extracted *Amaranthus caudatus* extract should be an alternative chlorophyll source for DSSC preparation in geographical regions that *Amaranthus caudatus* is widely available. Overall, natural dyes as sensitizers of DSSCs are promising because of their environmental friendliness, low-cost production and simple and energy-efficient manufacturing.

6. REFERENCES

[1] N. S. Lewis, Science 315 (2007) 798.

[2] A. Fujishima, K.Honda, Nature 238 (1972) 37.

[3] H. Gerischer, F.Willig, Top. Curr. Chem. 61 (1976) 31.

[4] R. Memming, Semiconductor Electrochemistry, Wiley-VCH Verlag GmbH, Weinheim, 2001.

[5] B. Oregan, M. Gratzel, Nature 353 (1991) 737.

[6] M. K. Nazeeruddin, A. Kay, I. Rodicio, R. Humphry-Baker, E. Muller, P. Liska, N. Vlachopoulos, M. Gratzel, J. Am. Chem. Soc.115 (1993) 6382.

[7] D. Matthews, P. Infelta, M. Grätzel, Sol. Energy Mater. Sol. Cells 44 (1996) 119.

[8] D. Cahen, G. Hodes, J. Phys. Chem. B 104 (2000) 2053.

[9] A. Hagfeldt, M. Grätzel, Chem. Rev. 95 (1995) 49.

[10] F. Pichot, B. A. Gregg, J. Phys. Chem. B 104 (2000b) 6.

[11] A. Hagfeldt, M. Grätzel, Acc. Chem. Res. 33, 5 (2000) 269.

[12] S. Nakade, T. Kanzaki, S. Yanagida, J. Phys. Chem. B 109 (2005) 3480.

[13] A.J. Frank, N. Kopidakis, J. van de Lagemaat, Coord. Chem. Rev. 248 (2004) 1165.

[14] S. Nakade, Y. Saito, S. Yanagida, J. Phys. Chem. B 107 (2003) 8607.

[15] A. Hagfeld, M. Gratzel, Chem. Rev. 95 (1995) 49.

[16] H. Rensmo, H. Lindstrom, S.-E. Lindquist, J. Electrochem. Soc. 143 (1996) 3173.

[17] I. A. Shkrob, M.C. Sauer, J. Phys. Chem. B 108 (2004) 12497.

[18] A. Zaban, A. Meier, B. Gregg, J. Phys. Chem. B 101 (1997) 7985.

[19] S. E. Koops, B.C. O'Regan, P. R. F. Barnes,J. R. Durrant, J. Am. Chem. Soc.131 (2009) 4808.

[20] S. Pelet, J. E. Moser, M. Gratzel, J. Phys. Chem. B 104 (2000) 1791.

[21] J. N. Clifford, E. Palomares, M. K. Nazeeruddin, M. Gratzel, J. R. Durrant, J. Phys. Chem. C 111 (2007) 6561.

[22] K. Miettunen, J. Halme, M. Toivola, P. Lund, J. Phys. Chem. C 112 (2008) 4011.

[23] M. Toivola, F. Ahlskog, P. Lund, Sol. Energy Mater. Sol. Cells 90 (2006) 2881.

[24] Y. Jun, J. Kim, M. Kang, Sol. Energy Mater. Sol. Cells 91 (2007) 779.

[25] L. Ke, S. Dolmanan, L. Shen, P. Pallathadk, Z. Zhang, D. Lai, H. Liu, Sol. Energy Mater. Sol. Cells 94 (2010) 323.

[26] Z. Zhang, S. Zakeeruddin, B. O'Regan, R. Humphry-Baker, M. Grätzel, J. Phys. Chem. B 109 (2005) 21818.

[27] P. Wang, S. Zakeeruddin, M. Grätzel, J. Chem. 125 (2004) 1241.

[28] G. Kumara, A. Konno, K. Shiratsuchi, J. Tsukahara, K. Tennakone, Chem. Mater. 14 (2002) 954.

[29] V. Perera, M. Senevirathna, P. Pitigala, K. Tennakone, Sol. Energy Mater. Sol. Cells 86 (2005) 443.

[30] J. Krüger, R. Plass, M. Grätzel, H- J Matthieu, Appl. Phys. Lett. 81 (2002) 367.

[31] A. O'Mahony, D. Silvester, L. Aldous, C. Hardacre R. Compton, J. Chem. Eng. Data 53 (2008) 2884.

[32] N. Papageorgiou, W. Maier, M. Grätzel, J. Electrochem. Soc. 144 (1997) 876.

[33] T.Murakami,M. Grätzel, Inorganica Chimica Acta 361 (2008) 572.

[34] Tsung-Wei Lin, Jun-Ren Lin, Sheng-You Tsai, Jing-Nang Lee, Chen-Ching Ting, The 31st National Conference on Theoretical and Applied Mechanics, December 21-22, 2007.

[35] M. Grätzel, J. Photochem. Photobiol. A: Chem. 164 (2004) 3.

[36] M. K. Nazeeruddin, S. M. Zakeeruddin, R. Humphry-Baker, M. Jirousek, P. Liska, N. Vlachopoulos, V. Shklover, C.H. Fischer, M. Gratzel, Inorg. Chem. 38 (1999) 6298.

[37] M. K. Nazeeruddin, P. Pechy, M. Gratzel, Chem. Commun. (1997) 1705.

[38] P. Wang, C. Klein, R. Humphry-Baker, S. M. Zakeeruddin, M. Gratzel, J. Am. Chem. Soc.127 (2005) 808.

[39] D. B. Kuang, C. Klein, S. Ito, J. E. Moser, R. Humphry-Baker, N. Evans, F. Duriaux, C. Graetzel, S. M. Zakeeruddin, M. Graetzel, Adv. Mater. 19 (2007) 1133.

[40] K. Hara, T. Sato, R. Katoh, A. Furube, Y. Ohga, A. Shinpo, S. Suga, K. Sayama, H. Sugihara, H. Arakawa, J. Phys. Chem. B 107 (2003) 597.

[41] Z. S.Wang, Y. Cui, K. Hara, Y. Dan-Oh, C. Kasada, A. Shinpo, Adv. Mater.19 (2007) 1138.

[42] Sigrid Hedbor, Linn´ea Klar, Master Thesis ,2005, UPTEC W 05-016, ISSN 1401-5765.

[43] J.M. Kong, L. S. Chia, N. K. Goh, T. F. Chia, R. Brouillard, Phytochemistry 64 (2003) 923.

[44] R. Brouillard, Chemical structure of anthocyanins, In Anthocyanins as food colors, P. Markakis, ed. (New York: Academic Press) (1982) 1.

[45] D. Strack, T. Vogt, W. Schliemann, Photchem. 62 (2003) 247.

[46] Y. Cai, M. Sun, W. Schliemann, H. Corke, J. Agr. Food. Chem.49 (2001) 4429.

[47] H. Ishikita , W. Saenger, J. Biesiadka, B. Loll, EW. Knapp , Proc. Natl. Acad. Sci. U.S.A. 103 (2006) 9855.

[48] H. Tamiaki, R. Shibata and T. Mizoguchi, *Photochem. Photobiol.*83 (2007) 152.

[49] M.A. Green, Solar cell, operating principle, technology and system application, Prentice-Hall, Inc. Englewood Cliffs (1998).

[50] L. Fan, S. Kang, J. Wu, S. Hao;, Z. Lan, J. Lin, Energ. Sources 32 (2010) 1559.

[51] G. Calogero, G. Di Marco, S. Cazzanti, S. Caramori, R. Argazzi, A. Di Carlo, C. A. Bignozzi, I. J. Mol. Sci. 11 (2010) 254.

[52] F. Aqil, I. Ahmad, World J. Microbiol. Biotechnol. 19 (2003) 653.

[53] J. Cherepy, G P. Smestad, M. Grätzel, JZ.Zhang, J. Phys. Chem. B 101 (1997) 9342.

[54] H. Zhou, L. Wu, Y. Gao, T. Ma, J. Photochem. Photobiol. A: Chem. 219 (2011) 188.

[55] K. Sayama, S. Tsukagoshi, T. Mori, K. Hara, Y. Ohga, A. Shipou,Y. Abe, S. Suga, H.Arakawa, Sol. Energy Mater. Sol. Cells 80 (2003) 47.

[56] A. Kay, R. Humphry-Baker, M. Grätzel, J. Phys. Chem. 98 (1994) 952.

[57] K. Kalyanasundaram,N. Vlachopoulos, V. Krishnan, A. Monnier, M. Grätzel, J. Phys. Chem. 91 (1987) 2342.

[58] S. Hao, J. Wu, Y. Huang, J. Lin, Sol. Energy 80 (2006) 209.

[59] K. Wongcharee, V. Meeyoo, S. Chavadej, Sol. Energy Mater. Sol. Cells 91(2007) 566.

[60] G.R.A. Kumara, S. Kanebo, M. Okuya, B. Onwona-Agyeman, A. Konno, K. Tennakone, Sol. Energy Mater. Sol. Cells 90 (2006)1220.

[61] Z. - S. Wang, H. Kawauchi, T. Kashime, H. Arakawa, Coord. Chem. Rev. 248 (2004)1381.